cells

MDPI

Article

Cyclosporin A Increases Mitochondrial Buffering of Calcium: An Additional Mechanism in Delaying Mitochondrial Permeability Transition Pore Opening

Jyotsna Mishra [1], Ariea J. Davani [1], Gayathri K. Natarajan [1], Wai-Meng Kwok [1,2,3,4], David F. Stowe [1,2,5,6] and Amadou K.S. Camara [1,2,4,6,*]

1 Department of Anesthesiology, Medical College of Wisconsin, Milwaukee, WI 53226, USA
2 Cardiovascular Center, Medical College of Wisconsin, Milwaukee, WI 53226, USA
3 Department of Pharmacology and Toxicology, Medical College of Wisconsin, Milwaukee, WI 53226, USA
4 Cancer Center, Medical College of Wisconsin, Milwaukee, WI 53226, USA
5 Research Service, Zablocki VA Medical Center, Milwaukee, WI 53295, USA
6 Department of Physiology, Medical College of Wisconsin, Milwaukee, WI 53226, USA
* Correspondence: aksc@mcw.edu; Tel.: +1-(414)-955-5624

Received: 6 July 2019; Accepted: 3 September 2019; Published: 7 September 2019

Abstract: Regulation of mitochondrial free Ca^{2+} is critically important for cellular homeostasis. An increase in mitochondrial matrix free Ca^{2+} concentration ($[Ca^{2+}]_m$) predisposes mitochondria to opening of the permeability transition pore (mPTP). Opening of the pore can be delayed by cyclosporin A (CsA), possibly by inhibiting cyclophilin D (Cyp D), a key regulator of mPTP. Here, we report on a novel mechanism by which CsA delays mPTP opening by enhanced sequestration of matrix free Ca^{2+}. Cardiac-isolated mitochondria were challenged with repetitive $CaCl_2$ boluses under Na^+-free buffer conditions with and without CsA. CsA significantly delayed mPTP opening primarily by promoting matrix Ca^{2+} sequestration, leading to sustained basal $[Ca^{2+}]_m$ levels for an extended period. The preservation of basal $[Ca^{2+}]_m$ during the $CaCl_2$ pulse challenge was associated with normalized NADH, matrix pH (pH_m), and mitochondrial membrane potential ($\Delta\Psi_m$). Notably, we found that in PO_4^{3-} (P_i)-free buffer condition, the CsA-mediated buffering of $[Ca^{2+}]_m$ was abrogated, and mitochondrial bioenergetics variables were concurrently compromised. In the presence of CsA, addition of P_i just before pore opening in the P_i-depleted condition reinstated the Ca^{2+} buffering system and rescued mitochondria from mPTP opening. This study shows that CsA promotes P_i-dependent mitochondrial Ca^{2+} sequestration to delay mPTP opening and, concomitantly, maintains mitochondrial function.

Keywords: cyclosporin A; mitochondria calcium buffering; mitochondria bioenergetics; mitochondria permeability transition pore; inorganic phosphate

1. Introduction

Regulation of intra-mitochondrial free calcium ($[Ca^{2+}]_m$) is critical in cardiac physiology and pathophysiology. Under physiological conditions, a moderate increase in $[Ca^{2+}]_m$ is believed to stimulate key enzymes of the Krebs cycle and oxidative phosphorylation and to drive mitochondrial ATP production to match cellular energy demand [1,2]. In contrast, a pathological increase in $[Ca^{2+}]_m$ causes opening of the mitochondrial permeability transition pore (mPTP), a key factor in initiation of cell death [3,4]. Pathophysiological dysregulation of $[Ca^{2+}]_m$ is a primary mediator in cardiac ischemia and reperfusion (IR) injury, as Ca^{2+} overloading can lead to apoptosis [5–7].

$[Ca^{2+}]_m$ is regulated by a dynamic balance between mitochondrial Ca^{2+} uptake, intra-mitochondrial Ca^{2+} buffering, and mitochondrial Ca^{2+} release. Mitochondrial Ca^{2+} uptake

is mediated primarily through the mitochondrial Ca^{2+} uniporter (MCU) [8–10], and is controlled by the large membrane potential ($\Delta\Psi_m$: −180 to −200 mV) across the inner mitochondrial membrane (IMM). The $\Delta\Psi_m$ in turn is generated by the flow of electrons and proton pumping along the respiratory chain complexes [11]. When $[Ca^{2+}]_m$ increases, this depolarizes $\Delta\Psi_m$, which is compensated by enhanced H^+ pumping/extrusion to alkalinize the matrix. Therefore, powerful, dynamic buffering of matrix pH (pH_m) and Ca^{2+} are required to enable sufficient recovery of $\Delta\Psi_m$ and to avoid overloading the matrix with a high $[Ca^{2+}]$. Inorganic phosphate (P_i) has been recognized as a major player in maintaining the trans-matrix pH gradient when accompanied by the effective cotransport of H^+ [12] and buffering of matrix Ca^{2+} through the formation of amorphous calcium phosphate (Ca–P_i) granules [13–15]. The Ca–P_i buffer system sets the free Ca^{2+} at a steady-state level, enabling greater mitochondrial Ca^{2+} loading without impeding the Ca^{2+} uptake and affecting the efflux system [16–18]. The efflux systems that regulate $[Ca^{2+}]_m$ are the Na^+/Ca^{2+}exchanger (NCLX) [17], and the putative Na^+-independent Ca^{2+} exchanger/Ca^{2+}-hydrogen exchanger (CHE) [19]. Any disruption in the uptake, and or impairment in the buffering or efflux of Ca^{2+} would disrupt the delicate balance of the $[Ca^{2+}]_m$ and lead to impaired bioenergetics and to opening of the mPTP [3,4].

The opening of the high conductance mPTP channel is associated with a high degree of mitochondrial swelling, dissipation of $\Delta\Psi_m$, uncoupling of oxidative phosphorylation, membrane rupture and release of sequestered Ca^{2+}, metabolites, and apoptotic signaling molecules [20–23]. Although the molecular components of the mPTP and its regulation remain largely unclear, cyclophilin D (Cyp D) is the only unambiguously recognized regulatory component of the mPTP. Cyp D is a mitochondrial matrix peptidyl-prolyl cis-trans isomerase (PPIase) that is translocated to the IMM during high matrix Ca^{2+} conditions; Cyp D is proposed to facilitate conformational changes in the putative mPTP core proteins thereby regulating pore opening [24–26].

Adenine nucleotides (AdN: ATP and ADP) have been implicated in the inhibition of Ca^{2+}-dependent mPTP opening [27,28]. A previous study from our laboratory suggested that matrix AdN modulate $[Ca^{2+}]_m$, potentially by increased buffering of $[Ca^{2+}]_m$ [29]. Oligomycin (OMN), an F_0F_1-ATP synthase inhibitor, influences the AdN (ATP/ADP) pool, and has been shown to modulate mPTP opening [30]. Cyclosporin A (CsA), a potent mPTP inhibitor is also believed to suppress pore opening by inhibiting matrix Cyp D, thereby preventing the Cyp D-induced conformational changes in mPTP core proteins [31,32]. CsA has long been known to desensitize mPTP from early opening during Ca^{2+} challenges by impeding Ca^{2+} interaction with Cyp D; however, the direct effects of CsA on the $[Ca^{2+}]_m$ buffering system have not been investigated systematically. It is worth noting that in a previous study from Chalmers and Nicholls [14], it was proposed that CsA enhances the Ca^{2+} loading capacity of mitochondria without changing the relationship between free $[Ca^{2+}]_m$ and total $[Ca^{2+}]_m$ during continuous Ca^{2+} infusion in isolated rat liver and brain mitochondria. Altschuld et al. [33] proposed that CsA increases mitochondrial Ca^{2+} influx and reduces its efflux. Later, Wei et al. [34] demonstrated that although CsA had no effect on MCU activity, it inhibited NCLX activity at higher concentrations. Altogether, these findings raise important questions about how CsA delays Ca^{2+}-induced mPTP opening while increasing net $[Ca^{2+}]_m$ accumulation. Our study sought to answer these questions by (i) examining the effect of CsA during repeated $CaCl_2$ challenges over an extended time-period on mitochondrial Ca^{2+} buffering, and (ii) by examining the underlying changes in bioenergetics during excessive Ca^{2+} overload.

To address our objective, we investigated systematically the effect of CsA on mitochondrial Ca^{2+} buffering and compared its effect with a known matrix buffering component, the AdN pool (OMN+ADP), by monitoring $[Ca^{2+}]_e$, $[Ca^{2+}]_m$, and key mitochondrial bioenergetics variables, $\Delta\Psi_m$, pH_m, and NADH (redox state), under conditions of repeated Ca^{2+} loading. Furthermore, we determined the effect of CsA on the rescue of buffering capability and bioenergetics of failing mitochondria just before mPTP opening. We found that CsA enhanced the sequestration of mitochondrial Ca^{2+}, maintained $[Ca^{2+}]_m$ at a steady-state level, and markedly delayed mPTP opening. In addition, CsA preserved $\Delta\Psi_m$, NADH, and pH_m during $CaCl_2$ bolus challenges. However, in the absence of P_i, this

CsA-induced matrix Ca^{2+} sequestration was abrogated, and in turn led to the early mPTP opening. The results described herein reveal a novel way by which CsA modulates matrix Ca^{2+} sequestration to maintain $[Ca^{2+}]_m$, despite increased Ca^{2+} loading. CsA-mediated Ca^{2+} sequestration is likely achieved via a P_i-dependent $[Ca^{2+}]_m$ buffering system that delays Ca^{2+}-induced mPTP opening.

2. Materials and Methods

2.1. Materials

All chemical reagents were purchased from Sigma-Aldrich (St. Louis, MO, USA), unless stated otherwise. Fluorescent probes Fura-4F, Fura-$4F^{AM}$, tetramethylrhodamine methyl ester perchlorate (TMRM) and 2′,7′-Bis-(2-Carboxyethyl)-5-(and-6)-carboxyfluorescein, acetoxymethyl ester ($BCECF^{AM}$) were purchased from Life Technologies (Eugene, OR, USA).

2.2. Animals

Albino Hartley guinea pigs of both sexes weighing between 250 to 350 g were procured from Kuiper Rabbit Farm (Gary, IN, USA). All procedures were carried out in accordance with the National Institutes of Health (NIH) Guide for the Care and Use of Laboratory Animals (NIH Publication No. 85-23, revised 1996) and were approved by the Institutional Animal Care and Use Committee of the Medical College of Wisconsin.

2.3. Mitochondria Isolation

Mitochondria were isolated from guinea pig hearts as described previously [29,35,36]. Briefly, the guinea pig was anesthetized with an intraperitoneal injection of 30 mg ketamine plus 700 units of heparin, for anticoagulation, and the heart was rapidly excised and minced in ice-cold isolation buffer containing 200 mM mannitol, 50 mM sucrose, 5 mM KH_2PO_4, 5 mM MOPS, 1 mM EGTA, and 0.1% bovine serum albumin (BSA) at pH 7.15 (adjusted with KOH). The suspension was homogenized at low speed for 20 s in ice-cold isolation buffer containing 5 U/mL protease (from *Bacillus licheniformis*) and the homogenate was centrifuged at 8000× *g* for 10 min. The supernatant was discarded, and the pellet was suspended in 25 mL isolation buffer, and centrifuged at 850× *g* for 10 min. The supernatant was centrifuged further at 8000× *g* to yield the final mitochondrial pellet, which was suspended in isolation buffer and kept on ice until experimentation. All isolation procedures were performed at 4 °C and all experiments were conducted at room temperature. Protein concentration was determined by the Bradford method and the final mitochondrial suspension was adjusted to 12.5 mg protein/mL with isolation buffer.

The functional integrity of mitochondria was determined by the respiratory control index (RCI) as described before [29,37]. Mitochondria were energized with pyruvic acid (PA, 0.5 mM; pH 7.15, adjusted with KOH) followed by ADP (250 µM) addition. RCI was defined as the ratio of state 3 (after added ADP) to state 4 respiration (after complete phosphorylation of the added ADP). Only mitochondrial preparations with RCIs ≥ 10 were used to conduct further experiments.

2.4. Experimental Groups and Protocols

Two protocols (Protocol A and Protocol B) were used to assess the effect of CsA and AdN on mitochondrial Ca^{2+} handling and bioenergetics in normal and Ca^{2+}-overloaded mitochondria, as shown in Figure 1. Protocol A investigated the ability of CsA and AdN to modulate mitochondrial Ca^{2+} handling and delay mPTP opening. To further substantiate CsA-mediated buffering of matrix Ca^{2+}, Protocol B was designed to test the effectiveness of CsA and AdN on rescuing a failing mitochondrial Ca^{2+} buffering system from imminent mPTP opening. There were five experimental groups: vehicle (DMSO), CsA, ADP, OMN, and OMN+ADP. Experiments were also conducted in the presence of deionized H_2O as another vehicle (not shown). Each group was subjected to two different experimental protocols (Protocol A and Protocol B) that differed in the order of treatment and addition of $CaCl_2$ boluses to the mitochondrial suspension in experimental buffer.

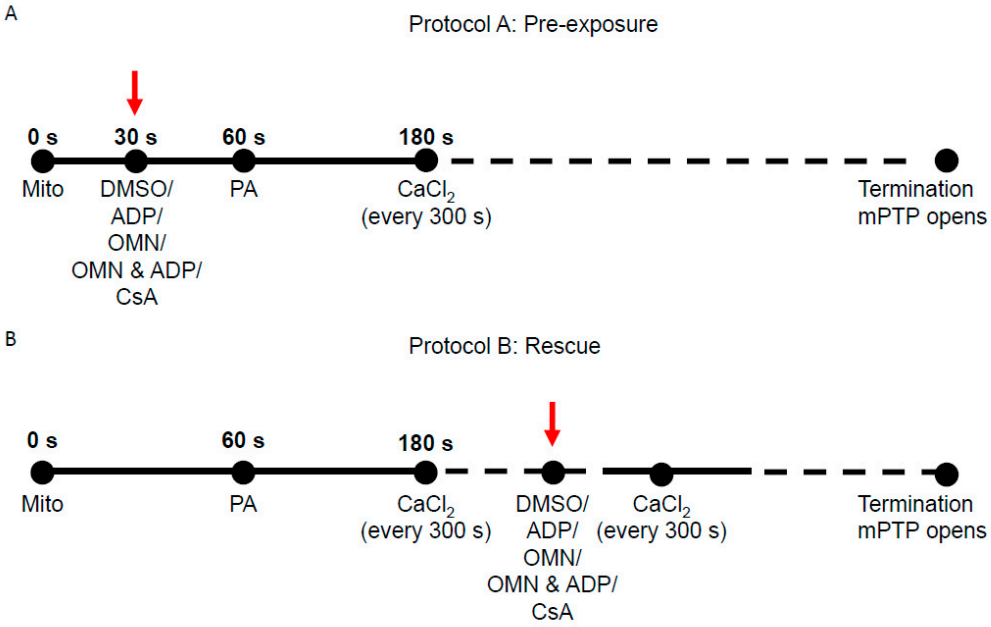

Figure 1. Schema of experimental timeline used to study the effect of Cyclosporin A (CsA) and adenine nucleotide (AdN) on mitochondrial Ca^{2+} handling and bioenergetics during repeated $CaCl_2$ pulses. (**A**) In Protocol A, at t = 0 s, mitochondria (mito, 0.5 mg) were added to the Na^+-free experimental buffer solution. The mitochondrial suspension was exposed to 0.5 μM CsA, 250 μM ADP, 10 μM oligomycin (OMN), or a combination of OMN+ADP at t = 30 s. Pyruvic acid (PA, 0.5 mM), was added at t = 60 s to energize mitochondria (state 2). At t = 180 s, 20 μM of $CaCl_2$ was added, followed by sequential additions of 20 μM $CaCl_2$ at every 300 s intervals until mPTP (mitochondrial permeability transition pore) opened or no further Ca^{2+} uptake was observed. (**B**) In Protocol B, the mitochondrial suspension was exposed to similar treatments as in Protocol A, but given after the last consecutive $CaCl_2$ bolus preceding the imminent onset of mPTP opening.

Delayed opening of mPTP (Protocol A): At t = 0 s, the experiment was initiated by suspending 0.5 mg of isolated mitochondria into the experimental buffer containing 130 mM KCl, 5 mM K_2HPO_4, 20 mM MOPS, 1 mM EGTA, 0.1% BSA, and EGTA ~0.036–0.040 μM at pH 7.15 (adjusted with KOH). At t = 30 s, mitochondria were treated with DMSO (1 μM), ADP (250 μM), OMN (10 μM), OMN+ADP or CsA (0.5 μM); at t = 60 s, mitochondria were energized with PA (0.5 mM). At t = 180 s, $CaCl_2$ bolus (20 μM final concentration) was added and subsequent $CaCl_2$ boluses added at 5 min intervals until pore opening (Figure 1A). Note that all experiments were conducted under state 2 conditions, except in the ADP-and OMN+ADP-treated groups.

Rescue of mitochondria from mPTP opening (Protocol B): The mitochondrial suspension was exposed to repetitive boluses of $CaCl_2$ (20 μM) as described in Protocol A; rescue of mitochondria from mPTP opening with the different treatments was carried out at 1 min of the last $CaCl_2$ bolus in which mitochondria Ca^{2+} uptake was observed before pore opening (Figure 1B). The onset of mPTP opening was predicted based on calcium retention capacity (CRC) of the DMSO (control)-treated group for each day's experiment. The pulse preceding mPTP opening observed in the control was the pulse chosen for targeted intervention in all subsequent experiments. In all experiments, extrusion of Ca^{2+} via the Na^+/Ca^{2+} exchanger (NCLX) was prevented by conducting all the experiments in Na^+-free conditions. That is, the respiration buffer, mitochondrial substrates, and all reagents/drugs were Na^+-free to prevent activation of the NCLX. Some experiments were conducted in the presence of 10 μM CGP 37157 (Tocris Bioscience), an NCLX inhibitor, which ascertained there was no potential Na^+ contamination in the respiration buffer from other sources [35,38,39].

2.5. Mitochondrial Function Measurements

Fluorescence spectrophotometry (Qm-8, Photon Technology International, Horiba, Birmingham, NJ, USA) was used to measure mitochondrial function, including mitochondria extra- and intra-matrix free $[Ca^{2+}]$ ($[Ca^{2+}]_e$ and $[Ca^{2+}]_m$, respectively), $\Delta\Psi_m$, redox state (NADH), and pH_m. Fura-4F penta-potassium salt (1 µM, Invitrogen™, Eugene, OR) was used to measure $[Ca^{2+}]_e$. For $[Ca^{2+}]_m$ measurements, mitochondria were incubated with Fura-4F AM (5 µM, Invitrogen™, Eugene, OR) for 30 min at room temperature (25 °C) followed by a final spin and resuspension to remove any residual dye. $\Delta\Psi_m$ was assessed using the cationic lipophilic dye TMRM (1 µM, Invitrogen™, Eugene, OR, USA) in a ratiometric excitation approach [40]. NADH was measured by tissue autofluorescence, and matrix pH (pH_m) was assessed by incubating mitochondria in 5 µM $BCECF^{AM}$ (Invitrogen, Carlsbad, CA, USA) for 30 min at room temperature (25 °C) followed by a final spin and resuspension [29,35,38,39].

2.6. Measurements of Free Ca^{2+}

Quantification of $[Ca^{2+}]_e$ and $[Ca^{2+}]_m$ were made using the fluorescent Ca^{2+} indicator probe Fura-4F with dual-excitation wavelengths (λ_{ex}) at 340/380 nm and a single emission wavelength (λ_{em}) at 510 nm. Ca^{2+} fluorescent intensities with Fura-4F are not influenced by background noise (e.g., NADH autofluorescence), so a background subtraction was unnecessary [38]. Fura-4F fluorescence ratios (F_{340}/F_{380}) were used to calculate $[Ca^{2+}]$ using the equation described by Grynkiewicz: [41].

$$[Ca^{2+}] = K_d \frac{S_{f2}}{S_{b2}} \frac{(R - R_{min})}{(R_{max} - R)}. \quad (1)$$

The K_d value for Fura-4F binding to Ca^{2+} is 890 nM, which was described by us previously [38]. R is the ratio of the fluorescence intensities at λ_{ex} 340 and 380 nm, S_{f2}/S_{b2} is the ratio of fluorescence intensities measured at λ_{ex} 380 nm in Ca^{2+}-free (f)/Ca^{2+}-saturated (Ca^{2+}-bound, b) conditions. R_{min} (Ca^{2+}-free) and R_{max} (Ca^{2+}-saturated) are R values for Fura 4F, carried out after mPTP opening, adding 1 mM $CaCl_2$, followed by 10 mM EGTA, pH 7.1. The free $[Ca^{2+}]$ in the buffer was calculated using an online version of MaxChelator program (http://www.stanford.edu/~{}cpatton/maxc.html) and accordingly, a standard curve was generated for the Fura-4F signal to the free $[Ca^{2+}]$ in the experimental solution by fitting to the Grynkiewicz equation, as described above in Equation 1 [41].

2.7. Calculation of Mitochondrial Ca^{2+} Buffering Capacity

The ability of mitochondria to sequester Ca^{2+} is an index of its Ca^{2+} loading capacity, without altering mitochondrial function. Here we calculated mitochondrial Ca^{2+} buffering capacity ($m\beta_{Ca}$) using the model described by Bazil et al. [42]. Briefly, experimental data for extra-and intra-matrix Ca^{2+} were fit with smooth trend curves satisfying the equation:

$$y(t) = p_1 + p_2 e^{\frac{(t-p_3)}{p_4}} + p_5 t, \quad (2)$$

where y(t) was either $[Ca^{2+}]_e$ or $[Ca^{2+}]_m$ at any given time, t. Global trend-fits were performed in MATLAB (Mathworks, Inc., MA) and parameters p_1 (offset value), p_2 (pre = exponential constant), p_3 (time lag), p_4 (decay time constant), and p_5 (steady-state slope) were estimated and optimized using the lsqnonlin and fmincon functions.

Mitochondrial Ca^{2+} buffering capacity for the second Ca^{2+} pulse (a cumulative of 40 µM added Ca^{2+}) was then calculated [42] as:

$$m\beta_{Ca} = -\beta_{Ca,e} V_r \frac{d[Ca^{2+}]_e}{dt} / \frac{d[Ca^{2+}]_m}{dt}, \quad (3)$$

where, $m\beta_{Ca}$, is the intra-mitochondrial Ca^{2+} buffering power, $\beta_{Ca,e}$ is the extra-mitochondrial Ca^{2+} buffering power determined by:

$$\beta_{Ca,e} = 1 + \frac{\partial[\text{CaEGTA}]_e}{\partial[Ca^{2+}]_e}. \quad (4)$$

Vr is the volume ratio of the extra-mitochondrial space and matrix space (~2000), $d[Ca^{2+}]_e/dt$ and $d[Ca^{2+}]_m/dt$ are the rates of change of extra-and intra-mitochondrial free $[Ca^{2+}]$, respectively. $d[Ca^{2+}]_e/dt$ and $d[Ca^{2+}]_m/dt$ were estimated by evaluating the analytical derivative of Equation (2) using parameter estimates obtained from the trend fits [42].

Trend fits for data in Figure S4 were performed in Origin 2017 (OriginLab Corporation, Northampton, MA, USA).

2.8. Measurement of $\Delta\Psi_m$, Redox State (NADH) and Matrix pH

Membrane potential was assessed by the dual-excitation ratiometric approach using the fluorescent dye, TMRM, as described by Scaduto and Grotyohann [40] and in our published work [35,38,39]. Fluorescence changes were determined by two excitations, λ_{ex} 546 and 573 nm, and a single emission λ_{em} 590 nm. The calculated ratio of λex 573/546 is proportional to $\Delta\Psi_m$ and has the advantage of a broader dynamic range when compared to a single wavelength technique. Changes in mitochondrial redox state (NADH) were determined by autofluorescence (i.e., by exciting the energized mitochondria at λ_{ex} 350 nm and collecting data at λ_{em} 456 nm). An increase in the signal reflects an increase in the redox ratio of NADH to NAD^+ (i.e., a shift to a more reduced state). Matrix pH was assessed using $BCECF^{AM}$ (5 μM) at λ_{ex} 504 nm and λ_{em} 530 nm. This fluorescent probe emits less fluorescence in an acidic environment, thus a decrease in signal indicates matrix acidification and an increase in signal indicates matrix alkalization [29].

2.9. Depletion of Endogenous Mitochondrial Phosphate

Given the important role of P_i in the mitochondrial Ca^{2+} buffering system [14,29], we tested the effect of P_i in CsA-induced mitochondrial Ca^{2+} buffering. Isolated cardiac mitochondria were depleted of endogenous P_i by pre-incubating mitochondria for 10 min at room temperature with 0.75 units/mL hexokinase, 1 mM glucose, 0.5 mM ADP, 1 mM $MgCl_2$, and 5 mM PA, as previously described [14,43,44].

2.10. Statistical Analyses

Data were transferred from PTI FelixGX (Version 3) into Microsoft® Excel® (2007). An unpaired Student's t-test was used to evaluate significant differences between means of CsA-treated versus DMSO- and AdN-treated groups on specific variables ($[Ca^{2+}]_m$, $[Ca^{2+}]_e$, $\Delta\Psi_m$, NADH, or pH_m) in both Protocols A and B. The final data of a specific variable were expressed as mean ± standard error (SE) over at least 4 replicates of the same variable ($n = 4$). Comparisons within and between groups were performed by one-way ANOVA (analysis of variance) with Tukey's post-hoc test to examine differences among individual groups. $p < 0.05$ (two-tailed) was considered significant. See Figure legends for statistical notations.

3. Results

3.1. Effect of CsA on Extra-Matrix Free $[Ca^{2+}]$

To determine the effect of CsA on matrix Ca^{2+} uptake, we measured $[Ca^{2+}]_e$ during repetitive additions of 20 μM $CaCl_2$ boluses at 5 min (300 s) intervals to allow characterization of the detailed kinetics of steady-state Ca^{2+} dynamics (influx and buffering). Figure 2 shows the dynamics of $[Ca^{2+}]_e$ during $CaCl_2$ pulse challenges, with different treatments. Panels A, B, C and panels D, E, F depict the Ca^{2+} dynamics profile using Protocols A and B, respectively. Each panel consists of five traces representing different treatment groups (DMSO, ADP, OMN, OMN+ADP, and CsA) in the presence of approximately 40 μM EGTA (carried over from the isolation buffer). In response to each $CaCl_2$ pulse, an increase in Fura-4F fluorescence intensity was observed, which then returned to a baseline; the

steady-state (ss) level is marked by the flat response as mitochondria take up and sequester the added Ca^{2+}. The opening of mPTP is evident by cessation of mitochondrial Ca^{2+} uptake and a sharp rise in the extra-matrix dye fluorescent intensity. Ca^{2+} concentrations were determined from the fluorescence ratios using Equation (1).

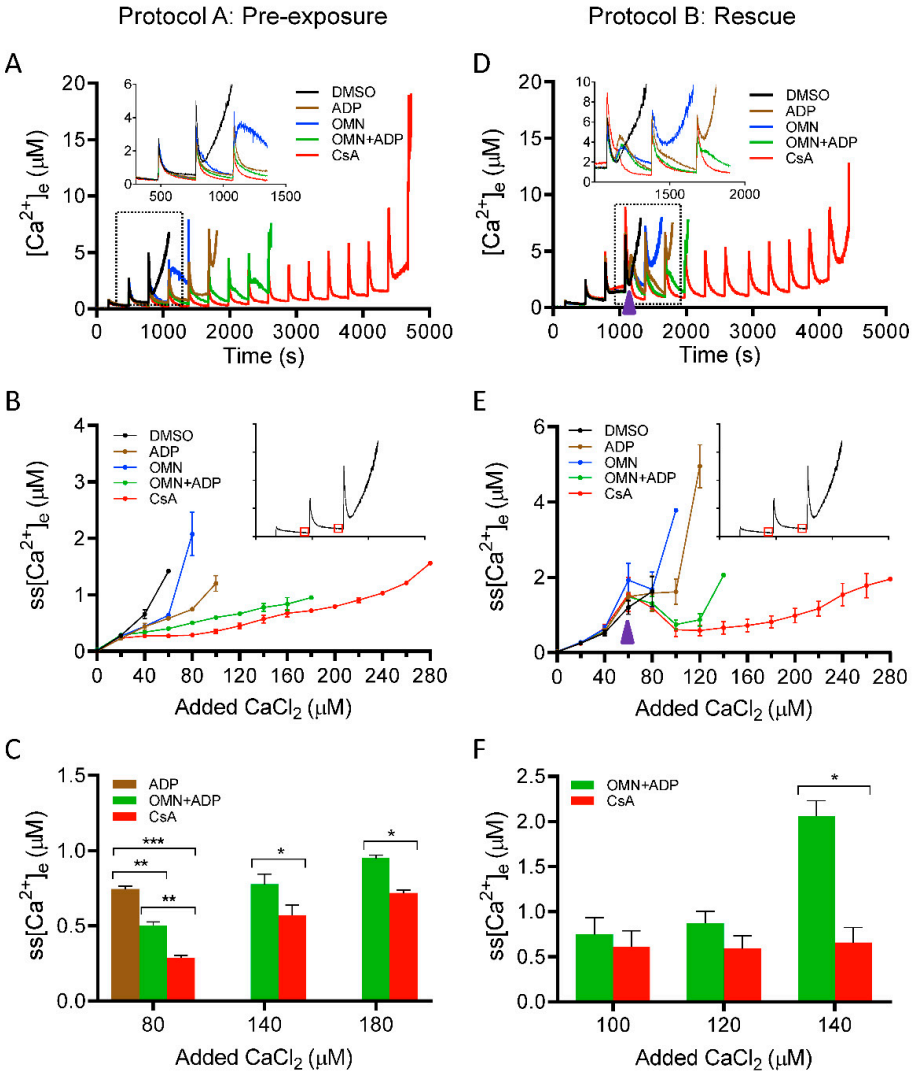

Figure 2. Effect of CsA and AdN on extra-mitochondrial calcium ($[Ca^{2+}]_e$) dynamics. Mitochondrial Ca^{2+} uptake and buffering for each of the treatment groups: DMSO (control; black trace), CsA (red trace), ADP (brown trace), OMN (blue trace), or OMN+ADP (green trace) are shown using the protocols depicted in Figure 1. Mitochondrial suspension was exposed to 0.5 μM CsA, 250 μM ADP, 10 μM OMN, or OMN+ADP before adding boluses of 20 μM $CaCl_2$ (Protocol A; left column). Mitochondrial suspension was exposed to added boluses of $CaCl_2$ (20 μM) and rescued mitochondria from mPTP opening (Protocol B; right column) with similar treatments as in Protocol A, at a time point at which it would initiate pore opening. Representative traces show change in extra-matrix free Ca^{2+} ($[Ca^{2+}]_e$) over time (**A**), and rescue of mitochondria from mPTP opening (**D**). Insets (**A**,**D**) show Ca^{2+} uptake kinetics in detail. Steady-state $[Ca^{2+}]_e$ ($ss[Ca^{2+}]_e$), 270 s after initiation of Ca^{2+} uptake, plotted as function of added Ca^{2+} (20 μM) every 300 s, in delay of mPTP opening (**B**), and rescue of mitochondria from mPTP opening (**E**). Insets (B,E) indicate the time points at which $ss[Ca^{2+}]_e$ was calculated. Quantification of steady-state $[Ca^{2+}]_e$ after a cumulative of 80, 140, and 180 μM $CaCl_2$ during delay of pore opening (**C**) and cumulative of 100, 120, and 140 μM $CaCl_2$ during rescue of mitochondria from mPTP opening (**F**). Error bars represent mean ± SEM (* $p < 0.05$; ** $p < 0.01$; *** $p < 0.005$). Arrowhead indicates time of addition of DMSO, ADP, OMN, OMN+ADP, or CsA during Protocol B.

We plotted steady-state $[Ca^{2+}]_e$ ($ss[Ca^{2+}]_e$) as a function of cumulative added $CaCl_2$ at each pulse (Figure 2B). The detailed dynamics of $ss[Ca^{2+}]_e$ for the initial four $CaCl_2$ pulses, in each group, are illustrated in the enlarged scale inset (Figure 2A). The exposure of mitochondria to DMSO and OMN, followed by repeated boluses of $CaCl_2$, resulted in a gradual increase in $ss[Ca^{2+}]_e$ with less mitochondrial Ca^{2+} uptake and rapid Ca^{2+} release by the third or fourth $CaCl_2$ pulse. The total CRC for the DMSO and OMN were comparable (i.e., 133.3 ± 13.3 nmol Ca^{2+}/mg protein and 146.6 ± 13.3 nmol Ca^{2+}/mg protein, respectively) (Figure S1). In the presence of ADP, mitochondria took up more Ca^{2+} before pore opening and the CRC was further augmented with OMN+ADP; the CRC value increased from 213.3 ± 13.3 nmol Ca^{2+}/mg protein for ADP alone to 373.3 ± 35.3 nmol Ca^{2+}/mg protein for OMN+ADP (Figure S1). Mitochondria treated with CsA before the addition of $CaCl_2$ boluses displayed a more robust Ca^{2+} uptake, with a significantly higher CRC value, 573.3 ± 26.6 nmol Ca^{2+}/mg protein, compared with all other groups (Figure 2A and Figure S1). Importantly, in CsA-treated mitochondria, the addition of $CaCl_2$ pulses (20 μM) did not significantly increase the $ss[Ca^{2+}]_e$ until the sixth to seventh pulse (Figure 2B), suggesting enhanced Ca^{2+} uptake. Figure 2C, summarizes the effects of the different treatments on the $ss[Ca^{2+}]_e$ for cumulative additions of 80, 140, and 180 μM of Ca^{2+}, which corresponds to the fourth, seventh, and ninth $CaCl_2$ pulses, respectively. The addition of CsA strongly blunted the Ca^{2+}-induced increase in $ss[Ca^{2+}]_e$ by stimulating faster and more Ca^{2+} uptake. We observed that the $ss[Ca^{2+}]_e$ was significantly lower for the CsA-treated mitochondria than for OMN+ADP-treated mitochondria after the cumulative addition of $CaCl_2$ of 80 μM (0.28 ± 0.0 μM vs. 0.50 ± 0.02 μM), 140 μM (0.57 ± 0.06 μM vs. 0.77 ± 0.06 μM), and 180 μM (0.71 ± 0.02 μM vs. 0.95 ± 0.1 μM) $CaCl_2$, respectively (Figure 2B,C). The sustained low $ss[Ca^{2+}]_e$ for an extended period of $CaCl_2$ additions in the CsA-treated group indicates a maintained $\Delta\Psi_m$ for Ca^{2+} uptake, resulting in enhanced Ca^{2+} loading capacity because of improved buffering.

We next examined $[Ca^{2+}]_e$ dynamics in the situation in which mitochondrial matrix Ca^{2+} nearly reached threshold, as determined by the predicted opening of mPTP; in this case we added CsA just before the anticipated mPTP opening. Using Protocol B (Figure 1), $[Ca^{2+}]_e$ was measured and the kinetics were compared in response to adding either DMSO, ADP, OMN, OMN+ADP, or CsA just before the onset of the mPTP opening (Figure 2D). The dynamic changes in $ss[Ca^{2+}]_e$ during the addition of different treatments are illustrated in more detail in the inset of Figure 2D. In the DMSO-treated mitochondria, three to four Ca^{2+} pulses (cumulative addition of 68 ± 4.9 μM $CaCl_2$) were sufficient to induce the release of matrix Ca^{2+}. Addition of ADP or OMN reversed the initial pore opening and delayed matrix Ca^{2+} release by one to two pulses compared to DMSO. Addition of OMN+ADP also showed a significant reversal of Ca^{2+} release with reduction in the $ss[Ca^{2+}]_e$ (0.74 ± 0.18 μM). Thus, there was a considerable increase in the CRC by OMN+ADP compared to DMSO (Figure 2D and Figure S1) and a further delay in mPTP opening by one additional $CaCl_2$ bolus compared to OMN or ADP alone. More impressively, the addition of CsA not only reversed the increasing trend of $ss[Ca^{2+}]_e$ to the baseline levels (0.42 ± 0.06 μM) (Figure 2D,E), it further maintained the $ss[Ca^{2+}]_e$ at a constant low value for an additional twelve to thirteen Ca^{2+} pulses. This resulted in a four-fold and a two-fold increase in the CRC, compared to DMSO and OMN+ADP, respectively (Figure 2E,F and Figure S1).

Altogether, these results demonstrate that CsA enhances mitochondrial Ca^{2+} uptake, thereby inhibiting a consequent increase in free $[Ca^{2+}]_e$ during $CaCl_2$ pulse challenges, leading to an increase in the CRC of the mitochondria. This sustained low $ss[Ca^{2+}]_e$ and concomitant increase in Ca^{2+} uptake are likely explained by enhanced $[Ca^{2+}]_m$ buffering to maintain basal $[Ca^{2+}]_m$, which results in a preserved $\Delta\Psi_m$ for Ca^{2+} uptake and greater CRC. To investigate further the potential for CsA on mediating Ca^{2+} buffering, it was necessary to examine the effects of CsA on matrix $[Ca^{2+}]_m$ dynamics in the next set of experiments.

3.2. *Effect of CsA on Matrix Free [Ca^{2+}] Handling*

Matrix Ca^{2+} was assessed with Fura-4 AM as described in Materials and Methods. We explored the effect of CsA on $[Ca^{2+}]_m$, under identical conditions and protocols as shown in Figure 1 (Protocols A,B). Mitochondrial Ca^{2+} buffering was measured as a function of a decrease in Ca^{2+} fluorescence, reaching

a steady-state at approximately 270 s after each bolus of $CaCl_2$ added. The magnitude of mitochondrial Ca^{2+} uptake for the first $CaCl_2$ pulse (20 μM) was similar in all groups; however, on subsequent additions of $CaCl_2$, the ADP- and/or OMN-treated groups showed faster declines in $[Ca^{2+}]_m$ with lower mitochondrial steady-state $[Ca^{2+}]_m$ ($ss[Ca^{2+}]_m$) and delayed mPTP opening compared to DMSO (Figure 3A,B). Interestingly, the CsA-treated group showed a small increase in $ss[Ca^{2+}]_m$ with each $CaCl_2$ pulse, but a gradual decline in $ss[Ca^{2+}]_m$ was observed after $[Ca^{2+}]_m$ exceeded 3 ± 0.10 μM with the cumulative addition of 100–150 μM $CaCl_2$ (Figure 3A,B) and a significant increase in CRC up to fifteen to sixteen pulses. This suggested that the buffering effect of CsA on matrix Ca^{2+} is triggered when $[Ca^{2+}]_m$ reaches a certain value.

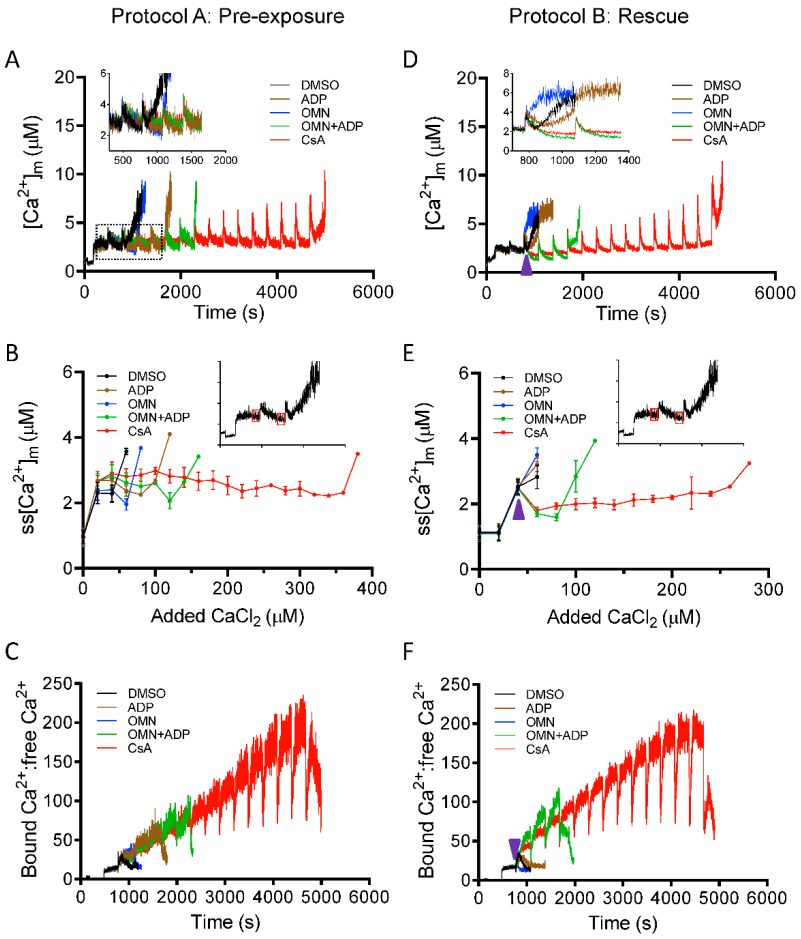

Figure 3. Effect of CsA and AdN on intra-matrix free Ca^{2+} ($[Ca^{2+}]_m$) dynamics. Mitochondrial Ca^{2+} uptake and buffering for each treatment groups, DMSO (control; black trace), CsA (red trace), ADP (brown trace), oligomycin (OMN, blue trace), or combination of OMN+ADP (green trace) are shown using the protocols depicted in Figure 1. Mitochondrial suspension was exposed to 0.5 μM CsA, 250 μM ADP, 10 μM OMN, or OMN+ADP before adding boluses of 20 μM $CaCl_2$ (Protocol A; left column). Mitochondrial suspension was exposed to added boluses of $CaCl_2$ (20 μM) and rescued from mPTP opening (Protocol B; right column) with similar interventions as in Protocol A, at a time point at which it would initiate mPTP opening. Representative traces show changes in $[Ca^{2+}]_m$ over time in delay of mPTP opening (**A**) and rescue of mitochondria from mPTP opening (**D**). Insets (A,D) show Ca^{2+} uptake kinetics in detail. Steady-state $[Ca^{2+}]_m$ ($ss[Ca^{2+}]_m$), 270 s after initiation of Ca^{2+} uptake, plotted as function of added Ca^{2+} (20 μM) every 300 s in delay of mPTP opening (**B**) and rescue of mitochondria from mPTP from opening (**E**). Insets (B,E) indicate the time points at which $ss[Ca^{2+}]_m$ was calculated. Change in matrix-bound Ca^{2+}:free Ca^{2+} over time in delay of mPTP opening (**C**) and rescue of mitochondria from mPTP opening (**F**). Arrowhead indicates time of addition of DMSO, ADP, OMN, OMN+ADP, or CsA during Protocol B.

To estimate the mitochondrial Ca^{2+} buffering capacity, the ratio of bound Ca^{2+}:free Ca^{2+} was calculated from the change in $[Ca^{2+}]_m$ (Figure 3A) to the total amount of Ca^{2+} taken up from the extra-matrix medium ($\Sigma Ca^{2+}{}_{uptake}$): ($\Sigma Ca^{2+}{}_{uptake}$-$[Ca^{2+}]_m$)/$[Ca^{2+}]_m$, as described previously [45]. Although the extent of bound Ca^{2+}:free Ca^{2+} at each Ca^{2+} pulse was comparable in all the treated groups (Figure 3C), the addition of CsA maintained the buffering capacity, with a gradual increase in the capacity to bind Ca^{2+} up to fifteen or sixteen Ca^{2+} pulses (Figure 3C).

Greater uptake of Ca^{2+} from the extra-matrix space (indicated by lower $ss[Ca^{2+}]_e$), combined with lower $ss[Ca^{2+}]_m$, indicated a greater Ca^{2+} buffering capacity of mitochondria in the presence of CsA. Consistent with this notion, the calculated matrix Ca^{2+} buffering capacity ($m\beta_{Ca}$) in CsA-treated mitochondria was about ten-fold higher compared to DMSO and two-fold higher than with OMN+ADP (Figure 4). This CsA-mediated increase in $m\beta_{Ca}$ is possibly due to an effect of CsA in triggering the matrix physiological buffers to enhance sequestration of Ca^{2+}.

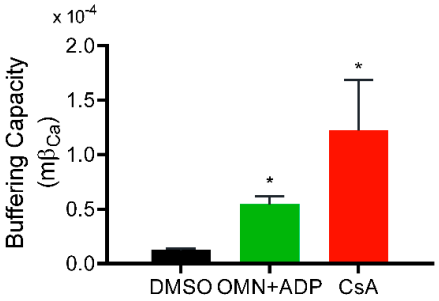

Figure 4. Effect of CsA and AdN on mitochondrial Ca^{2+} buffering capacity. Mitochondrial Ca^{2+} buffering capacity calculated from trend fits of $[Ca^{2+}]_e$ and $[Ca^{2+}]_m$ for DMSO-(control), CsA-, and OMN+ADP-treated mitochondria as described by Equations (2)–(4) in Materials and Methods. Buffering capacity for each treatment was calculated from three-five experiments each for $[Ca^{2+}]_e$ and $[Ca^{2+}]_m$ and averaged. Error bars represent mean ± SEM (* $p < 0.01$ compared with DMSO).

After observing the high buffering capacity of mitochondria pre-treated with CsA before the $CaCl_2$ bolus challenges, we next examined the effect of CsA on the rescue of mitochondria from Ca^{2+} release when the matrix Ca^{2+} buffering system (MCBS) becomes overwhelmed by the added boluses of $CaCl_2$ (Figure 1B). As shown in Figure 3D,E, OMN and ADP, each failed to reverse the mitochondrial Ca^{2+} efflux with added boluses; however, adding CsA or OMN+ADP at similar time points significantly reduced $ss[Ca^{2+}]_m$ by reinstating Ca^{2+} sequestration. This reversal was more effective and sustained in the presence of CsA than with OMN+ADP. This observation is consistent with the calculated values of bound Ca^{2+}: free Ca^{2+}, which increased two-fold for CsA compared to OMN+ADP (Figure 3F). Taken together, these data demonstrate that CsA increases the mitochondrial Ca^{2+} threshold for mPTP opening by activating $[Ca^{2+}]_m$ buffering that results in maintenance of a low $ss[Ca^{2+}]_m$.

3.3. Effect of CsA on Ca^{2+}-Mediated Changes in $\Delta\Psi_m$, NADH, and Matrix pH

A major driving force for Ca^{2+} uptake, in addition to the chemical gradient, is a high IMM potential gradient ($\Delta\Psi_m$); but increased Ca^{2+} uptake without efflux or sequestration can decrease $\Delta\Psi_m$ by flooding the matrix with positive charges. To strengthen the thesis that CsA increases the capacity of mitochondria to sequester Ca^{2+}, we next investigated the effect of CsA on mitochondrial bioenergetics. $\Delta\Psi_m$, NADH, and pH_m were assessed using the same protocols as described in Figure 1 for CRC to correlate changes in $[Ca^{2+}]_m$ to changes in bioenergetics over time. mPTP opening was marked by a sudden rise in the TMRM signal, indicating maximal depolarization of Ψ_m. Correspondingly, the oxidation of NADH was marked by a decrease in matrix NADH signal intensity when mPTP opens. Figure 5 shows representative traces of $\Delta\Psi_m$, NADH, and pH_m for each experimental condition. The rate of $\Delta\Psi_m$ depolarization and NADH oxidation correlated well with the induction of mPTP, as seen in the CRC data. The loss of CRC coincided with total $\Delta\Psi_m$

dissipation and NADH oxidation. DMSO-treated mitochondria (control) exhibited rapid Ca^{2+}-induced $\Delta\Psi_m$ depolarization and NADH oxidation (black trace) after only a few $CaCl_2$ pulses. Addition of OMN+ADP significantly delayed the Ca^{2+} induced $\Delta\Psi_m$ depolarization and NADH oxidation when compared to DMSO, with 533.3 ± 26.7 nmol Ca^{2+}/mg protein vs. 200 ± 23 nmol Ca^{2+}/mg protein and 546.7 ± 18.9 nmol Ca^{2+}/mg protein vs.173.3 ± 13.3 nmol Ca^{2+}/mg protein Ca^{2+} capacity, respectively (Figure 5A,B). Mitochondria treated with CsA maintained $\Delta\Psi_m$ and NADH for a higher number of $CaCl_2$ pulses than with OMN+ADP (666.7 ± 13.3 nmol Ca^{2+}/mg protein, and 626.6 ± 13.3 nmol Ca^{2+} /mg protein, respectively) (Figure 5A,B). Mitochondrial matrix pH (pH_m) is known to modulate mitochondrial P_i concentration and thus influence the matrix Ca^{2+} buffering [14]. The presence of CsA maintained pH_m at a basal level until mPTP opened (Figure 5C).

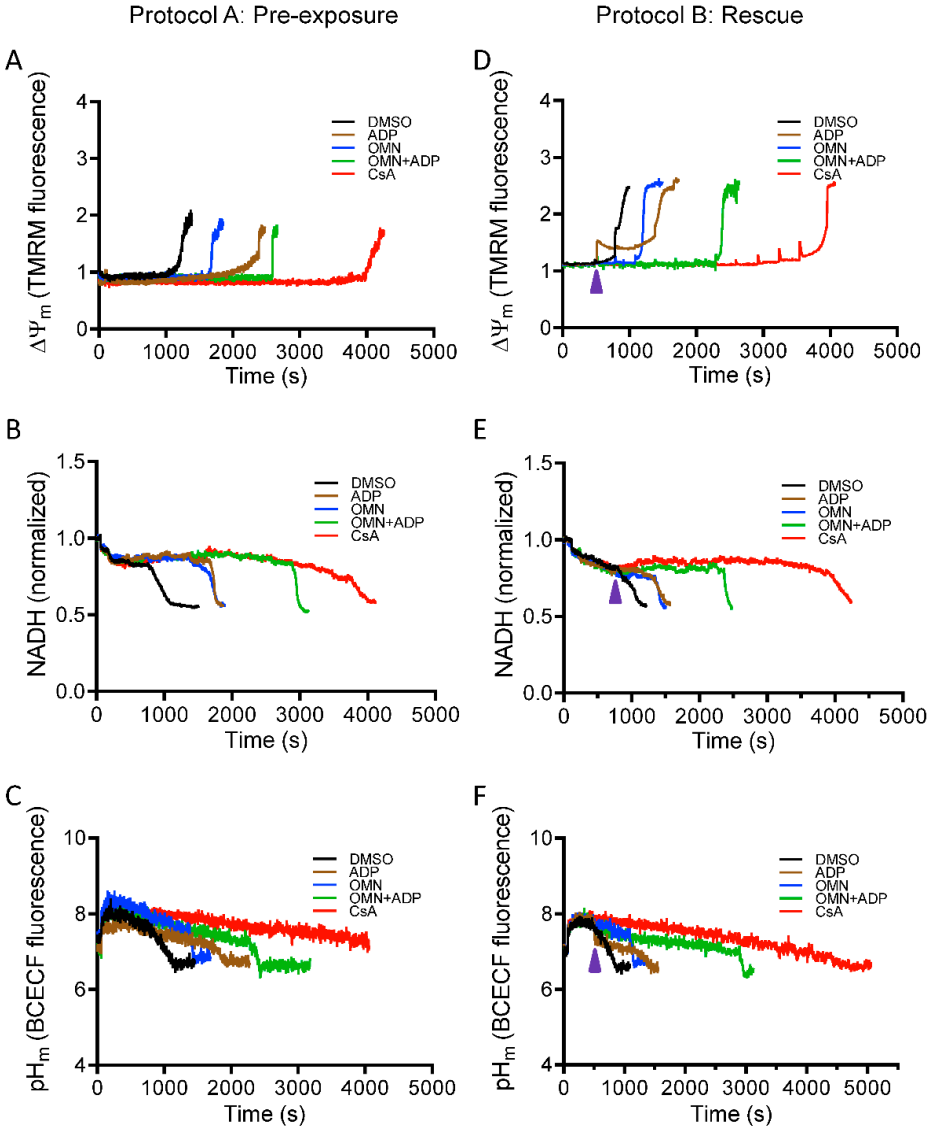

Figure 5. Effect of CsA and AdN on mitochondrial bioenergetics. The bioenergetic responses during Protocols A (left column) and B (right column) were monitored using the $\Delta\Psi_m$ sensitive dye TMRM (tetramethylrhodamine methyl ester perchlorate) (**A**,**D**), NADH autofluorescence (**B**,**E**), and pH_m-sensitive dye $BCECF^{AM}$ (2′,7′-Bis-(2-Carboxyethyl)-5-(and-6)-carboxyfluorescein, acetoxymethyl ester AM) (**C**,**F**). Purple arrowhead indicates time of addition of DMSO (1 µM), ADP (250 µM), OMN (10 µM), OMN+ADP, or CsA (0.5 µM) during Protocol B.

In Protocol B, intervention with OMN + ADP or CsA maintained $\Delta\Psi_m$, mitochondrial NADH, and pH_m (Figure 5D–F), and contributed to the improved capacity of mitochondria to take up and sequester additional Ca^{2+} after $CaCl_2$ pulses. However, OMN+ADP was less effective in preserving $\Delta\Psi_m$, NADH, and pH_m compared to CsA. This incapacity to sustain the bioenergetic status in the OMN+ADP- vs. CsA-treated mitochondria during $CaCl_2$ challenges reflects a lower capacity to sequester Ca^{2+} in the matrix for a protracted time.

In summary, maintenance of $\Delta\Psi_m$, NADH, and pH_m in the presence of CsA is consistent with changes in $[Ca^{2+}]_e$ and $[Ca^{2+}]_m$ that reflect greater Ca^{2+} sequestration (Figure S2) and uptake. Collectively, these results indicate that CsA reduced the accumulation of $[Ca^{2+}]_m$, by potentiating matrix Ca^{2+} buffering, which in turn, maintained $\Delta\Psi_m$, NADH, and pH_m necessary for normal mitochondrial function. Together, these mitochondrial variables preserve mitochondria and protect against mPTP opening.

3.4. Time Dependent Effect of CsA Addition on Rescue of Mitochondria from Imminent Ca^{2+}-Induced mPTP Opening

After demonstrating that CsA can reverse the induction of mPTP opening (Figures 2, 3 and 5), we next investigated the dynamics of $[Ca^{2+}]_e$, $[Ca^{2+}]_m$ and $\Delta\Psi_m$, by adding CsA at three different time points, before the onset of mPTP opening. This approach allowed us to determine the threshold at which CsA can effectively restore the mitochondrial sequestration system that will protect mitochondria from Ca^{2+} overload-mediated pore opening. Figure 6, panels A-C, show changes in $[Ca^{2+}]_e$, $[Ca^{2+}]_m$, and $\Delta\Psi_m$ depolarization, induced by adding CsA at 1, 2, and 3 min after the last $CaCl_2$ bolus in which mitochondrial Ca^{2+} uptake was observed before pore opened. Right panels D-F show detailed (close up) comparison of kinetics of $[Ca^{2+}]_e$, $[Ca^{2+}]_m$, and $\Delta\Psi_m$ after adding CsA at different time points. Adding CsA at all three tested time points, markedly delayed the large increase in $[Ca^{2+}]_e$ due to mitochondrial Ca^{2+} release. However, the effect of CsA to prolong Ca^{2+} uptake, which eventually maintains $ss[Ca^{2+}]_e$ at baseline, diminished as the interval before CsA addition and $[Ca^{2+}]_e$ accumulation was lengthened (Figure 6A). Adding CsA at 1 min caused a decline in $[Ca^{2+}]_e$, with a marked decrease in $ss[Ca^{2+}]_e$ (0.39 ± 0.07 μM) of the succeeding Ca^{2+} pulses, compared to adding CsA at 2 min (0.67 ± 0.03 μM) and 3 min (0.84 ± 0.05 μM) (Figure 6D; inset). In addition, we examined for changes in kinetics of $[Ca^{2+}]_m$ with CsA added at the same time points (Figure 6B). The rate of maximal Ca^{2+} buffering (i.e., the time to reach steady-state $[Ca^{2+}]_m$) and the Ca^{2+} threshold for pore opening was significantly higher when CsA was added at the early time points (i.e., 1 and 2 min) compared to the late time point of 3 min (Figure 6E, inset).

Next, in a parallel study, we monitored the corresponding changes in $\Delta\Psi_m$ profile at the same rescue time points (1, 2, or 3 min). Adding CsA reversed the Ca^{2+}-induced $\Delta\Psi_m$ depolarization even after a large depolarization (i.e., at 3 min; Figure 6C,F). Similar to its effect on $[Ca^{2+}]_e$ and $[Ca^{2+}]_m$, CsA restored and maintained $\Delta\Psi_m$ for a longer period at rescue points of 1 min vs. 2 and 3 min. Thus, at these points of intervention, CsA suppressed mPTP opening by increasing matrix Ca^{2+} buffering capacity, which maintained $\Delta\Psi_m$ and the driving force for further Ca^{2+} uptake (Figure 6C). Together, these results demonstrate that the magnitude of CsA-mediated increase in Ca^{2+} threshold for mPTP opening and maintenance of mitochondrial integrity is dependent on the $[Ca^{2+}]_m$ level before CsA intervention.

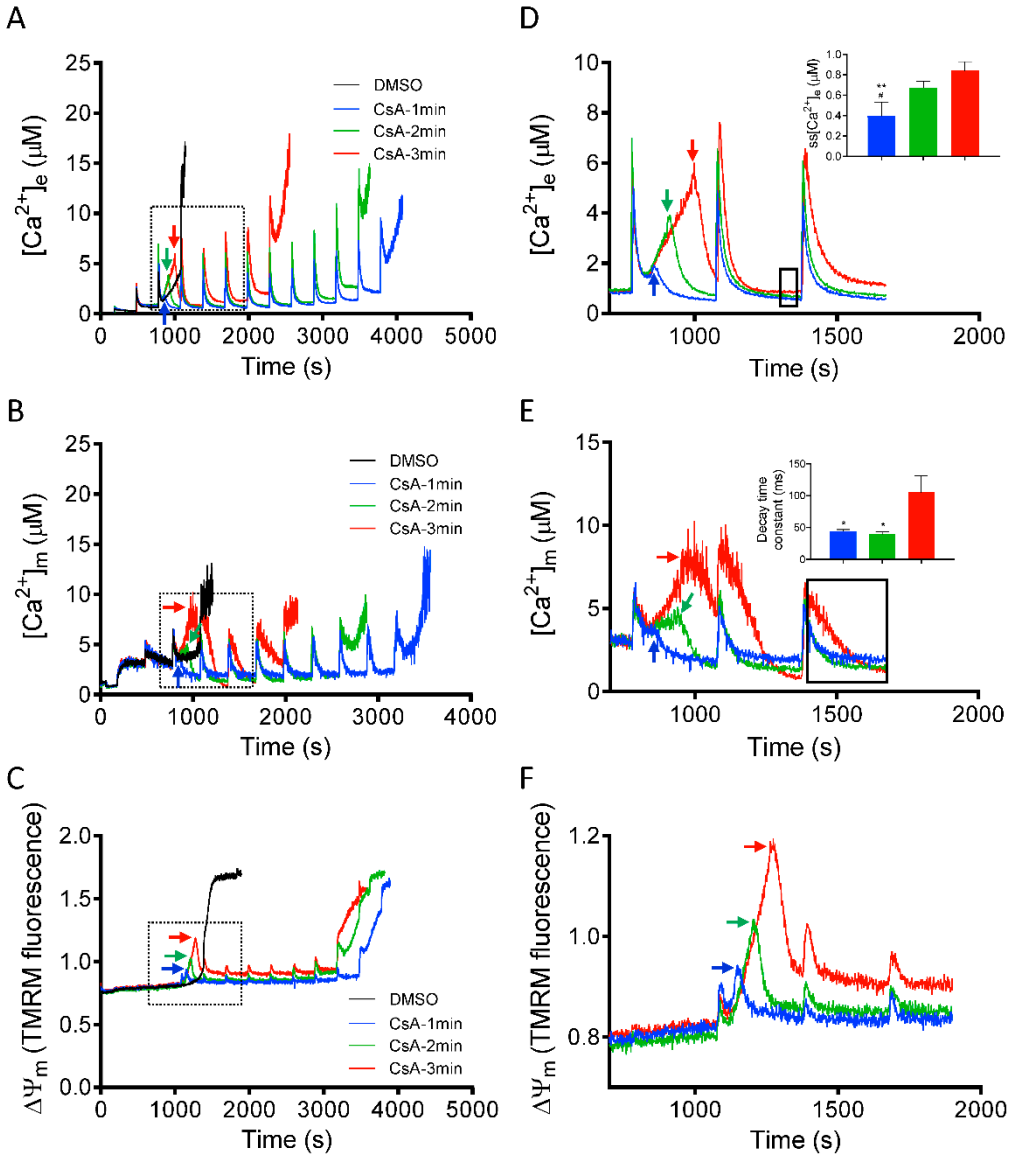

Figure 6. Time-dependent effects of CsA on mitochondrial Ca^{2+} dynamics and bioenergetics during rescue of mitochondria from mPTP opening. Changes in (**A**) extra-matrix free Ca^{2+} ($[Ca^{2+}]_e$), (**B**) intra-matrix free Ca^{2+} ($[Ca^{2+}]_m$) and (**C**) $\Delta\Psi_m$, when CsA was added at 1 min (blue trace), 2 min (green trace), and 3 min (red trace) after the last Ca^{2+} bolus before another Ca^{2+} bolus would have caused mPTP opening. Right panels show the effect of CsA on (**D**) $[Ca^{2+}]_e$, (**E**) $[Ca^{2+}]_m$, and (**F**) $\Delta\Psi_m$ dynamics during rescue of mitochondria from mPTP opening in greater detail. Insets (**D**,**E**) show relative ss$[Ca^{2+}]_e$ and decay time constant (ms) at specified time points (black dotted box), respectively. Arrows indicate time of addition of CsA (0.5 μM). Error bars represent mean ± SEM (* $p < 0.05$, ** $p < 0.01$ vs. 3 min and $^{\#}$ $p < 0.05$ vs. 2 min).

3.5. Role of Inorganic Phosphate in CsA-Induced $[Ca^{2+}]_m$ Regulation.

Inorganic phosphate (P_i) is a required component for mitochondrial matrix Ca^{2+} buffering [14,29]. To gain insight into the mechanism that underlies CsA-mediated activation of the MCBS, we monitored mitochondrial Ca^{2+} handling and $\Delta\Psi_m$ during repeated boluses of 20 μM $CaCl_2$ every 5 min, as described in Materials and Methods, but now in the absence of P_i. With mitochondria depleted of P_i, and in P_i-free media, the CRC of mitochondria treated with CsA before the $CaCl_2$ pulses was not different from DMSO (control). In addition, these mitochondria showed a gradual increase in ss$[Ca^{2+}]_e$ and interestingly, after cumulative additions of $CaCl_2$ to 80 ± 15 μM, there was a significant

decrease in mitochondrial Ca^{2+} uptake during additional $CaCl_2$ pulses (Figure 7A). These results implicated a P_i-dependent mechanism in the CsA-mediated delay in mPTP opening. In contrast, ADP and OMN+ADP, but not OMN alone, caused a significant delay in mPTP opening (Figure 7A) in the absence of P_i.

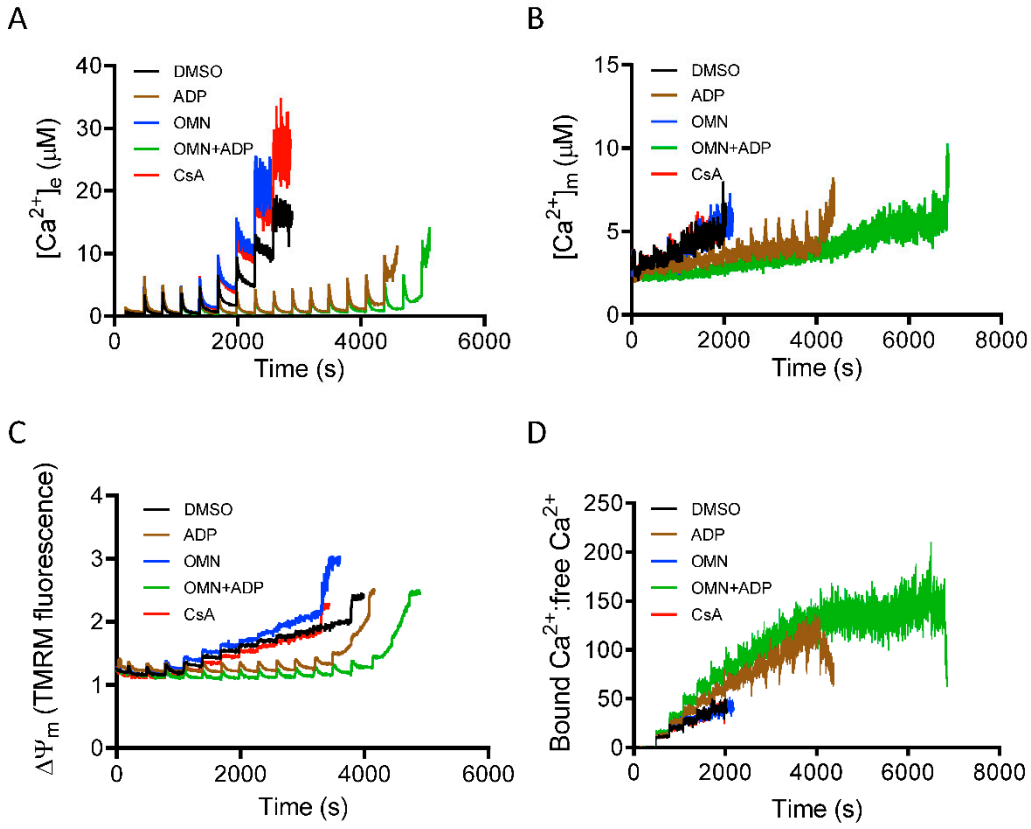

Figure 7. Effect of P_i on CsA-induced mitochondrial Ca^{2+} handling and bioenergetics. Time course of $[Ca^{2+}]_e$ (**A**), $[Ca^{2+}]_m$ (**B**), $\Delta\Psi_m$ (**C**), and matrix-bound Ca^{2+}:free Ca^{2+} (**D**) during consecutive additions of 20 μM $CaCl_2$ to a suspension of P_i-depleted mitochondria, pre-exposed to DMSO (control), CsA, ADP, OMN, or OMN+ADP.

Along with observing the P_i-mediated effect of CsA on $[Ca^{2+}]_e$ dynamics, we also measured $[Ca^{2+}]_m$ under identical conditions. In the absence of P_i, mitochondria showed a gradual increase in ss$[Ca^{2+}]_m$; matrix Ca^{2+} sequestration was strongly blunted in both DMSO-and CsA-treated groups. This reflected diminished buffering capacity with the increase in $[Ca^{2+}]_m$ (Figure 7B). However, in the presence of ADP and OMN+ADP in the P_i-depleted condition, mitochondria displayed robust CRC and enhanced Ca^{2+} buffering and thus decreased $[Ca^{2+}]_m$ (Figure 7B). Intriguingly, this effect was stronger than in the P_i replete condition (Figure 3). Mitochondria also showed an increased ratio of bound Ca^{2+}:free Ca^{2+} in the OMN+ADP-treated group, but not in the DMSO and CsA groups (Figure 7D). These data further support the premise that P_i is crucial in CsA-induced matrix Ca^{2+} buffering and P_i is a requisite component of matrix calcium sequestration.

Since we observed significant attenuation of Ca^{2+} uptake and buffering by CsA in the absence of P_i, we addressed how the altered mitochondrial Ca^{2+} dynamics impacted $\Delta\Psi_m$. Analysis of $\Delta\Psi_m$ in mitochondria depleted of P_i during $CaCl_2$ bolus challenges revealed a gradual depolarization with each Ca^{2+} pulse over time in the DMSO-, OMN-, and CsA-treated groups (Figure 7C); this was consistent with the low CRC in these three groups due to the poor buffering after additional $CaCl_2$ pulses. In contrast, mitochondria exposed to ADP or OMN+ADP in the P_i-depleted state exhibited restored and sustained $\Delta\Psi_m$, which supported a robust CRC (Figure 7C).

To further confirm the requisite role of P_i in mediating CsA-induced activation of the MCBS, a rescue experiment with 5 mM P_i was performed with DMSO-and CsA-treated groups in P_i-depleted condition. With addition of deionized H_2O (vehicle), pore opening was not prevented in either group (data not shown). The addition of exogenous P_i to the buffer triggered a rapid reversal of Ca^{2+} release (decrease in ($[Ca^{2+}]_e$) in parallel with complete restoration of $\Delta\Psi_m$ (Figure 8). In contrast, additional Ca^{2+} pulses in the P_i free DMSO-treated group failed to maintain ss$[Ca^{2+}]_e$ and basal Ψ_m, and induced rapid Ca^{2+} efflux (Figure 8). However, the CsA-treated mitochondria showed a robust uptake of $[Ca^{2+}]_e$ with low ss$[Ca^{2+}]_e$ and sustained $\Delta\Psi_m$ maintenance with additional $CaCl_2$ boluses (Figure 8). Taken together, these results establish that P_i is required for CsA-mediated mitochondrial Ca^{2+} buffering that maintains low $[Ca^{2+}]_m$ and preserves $\Delta\Psi_m$; this in turn contributes to the capacity for more Ca^{2+} uptake and thus increases the Ca^{2+} threshold for mPTP opening.

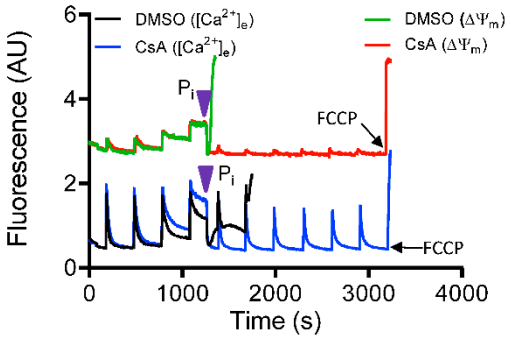

Figure 8. Mitochondrial Ca^{2+} modulation by CsA is phosphate (P_i)-dependent. Representative traces show change in extra-matrix Ca^{2+} fluorescence (Fura-4F Ratio) and $\Delta\Psi_m$ during consecutive 20 µM $CaCl_2$ boluses to induce mPTP opening in P_i-depleted mitochondria. P_i was added (purple arrowhead) at threshold point when mitochondria exhibited limited uptake of Ca^{2+} from the buffer.

4. Discussion

Matrix free $[Ca^{2+}]$ ($[Ca^{2+}]_m$) plays two important roles: (i) Activation of Ca^{2+}-dependent dehydrogenases for oxidative phosphorylation at low concentrations [46]; and (ii) regulation of cytosolic Ca^{2+} by sequestration of excess Ca^{2+} at high concentrations [47]. Excessive accumulation of free $[Ca^{2+}]_m$ is a leading factor in inducing mPTP opening. It is well established that repetitive mitochondrial Ca^{2+} loading triggers a gradual increase in $[Ca^{2+}]_m$, leading to a loss of IMM integrity that results in dissipation of $\Delta\Psi_m$ and release of Ca^{2+}. CsA is known to delay pore opening, in part, by inhibiting the PPIase activity of Cyp-D [31]. Whether CsA-mediated delay in mPTP opening involves regulation of $[Ca^{2+}]_m$ by P_i-induced matrix Ca^{2+} buffering has not been addressed before. In this study, we investigated the effects of CsA on $[Ca^{2+}]_m$ regulation during repeated Ca^{2+} loading and its functional significance in mPTP opening. Additionally, we determined if changes in $[Ca^{2+}]_m$ induced by CsA correlated with changes in mitochondrial bioenergetics under identical experimental conditions and if matrix P_i was required for the observed CsA effects.

Since the key postulate was that CsA contributes to mitochondrial Ca^{2+} buffering, all experiments were performed in Na^+-free condition to completely block NCLX as a route for efflux of excess matrix Ca^{2+}. This allowed us to directly assess mitochondrial Ca^{2+} buffering capacity under different treatments. Our major findings during repetitive $CaCl_2$ bolus challenges are: (i) CsA maintained basal ss$[Ca^{2+}]_m$ owing to increased mitochondrial Ca^{2+} buffering capacity; (ii) the effectiveness of CsA to maintain basal ss$[Ca^{2+}]_m$ correlates well with preserved mitochondrial bioenergetics; (iii) the buffering effect of CsA in a P_i-replete buffer was more pronounced than the known buffering effect of OMN+ADP; (iv) CsA-induced buffering was abolished in P_i-depleted mitochondria and P_i-free experimental medium. We conclude that the CsA-mediated delay in mPTP opening could, in large part, be attributed to CsA-induced activation of a P_i-dependent mitochondrial Ca^{2+} buffering system (MCBS), which maintains a low free $[Ca^{2+}]_m$ and preserves mitochondrial bioenergetics.

4.1. CsA-Mediated Inhibition of mPTP Opening Relates to the ss[Ca^{2+}]$_m$

Using the two protocols (Figure 1A,B), we examined the changes in [Ca^{2+}]$_e$ and [Ca^{2+}]$_m$ in response to boluses of $CaCl_2$ in the presence of vehicle (DMSO), CsA, ADP, OMN, or OMN+ADP over time. Our experimental approaches allowed us to define the contribution of CsA in the regulation of [Ca^{2+}]$_m$ when CsA was given before the $CaCl_2$ boluses (Protocol A) and at the threshold for pore opening under condition of increased free [Ca^{2+}]$_m$ accumulation (Protocol B). Our results clearly indicate that the effect of CsA on delaying mPTP opening is due largely to its efficacy in maintaining free ss[Ca^{2+}]$_m$ by activating the MCBS in a P_i-dependent manner, and thereby preclude early mitochondrial Ca^{2+} overload and delay induction of mPTP opening. Sustained low ss[Ca^{2+}]$_e$ in the CsA-treated group indicated increasing mitochondrial Ca^{2+} uptake driven by the enhanced sequestration of free [Ca^{2+}]$_m$ to maintain a transmembrane Ca^{2+} gradient and a charged $\Delta\Psi_m$ that facilitated additional Ca^{2+} uptake (Figure 2). Unlike previous studies [14,33,34], NCLX was blocked under our experimental conditions, to prevent Ca^{2+} efflux during the repetitive $CaCl_2$ additions; therefore, the net free ss[Ca^{2+}]$_m$ in our study was determined by the balance between Ca^{2+} uptake and Ca^{2+} sequestration.

Notably, the CsA-induced buffering of mitochondrial Ca^{2+} resulted in greater Ca^{2+} uptake to attain a steady-state, as shown by the gradual decrease in ss[Ca^{2+}]$_m$ with each added $CaCl_2$ pulse (Figure 3). Insofar as Ca^{2+}–P_i precipitation is a major mechanism for mitochondrial Ca^{2+} buffering, the sustained ss[Ca^{2+}]$_m$ after each $CaCl_2$ bolus indicated matrix Ca^{2+} storage, likely in the form of various inorganic Ca–P_i complexes [14]. The low and maintained ss[Ca^{2+}]$_m$ during continuous matrix Ca^{2+} uptake is consistent with formation of these complexes. Although our study did not provide direct experimental evidence for CsA-induced matrix Ca–P_i complex formation, the continuous rise in estimated bound Ca^{2+}:free Ca^{2+} ratio with each $CaCl_2$ bolus as well as the ten-fold increase in mβ_{Ca} clearly reflects a CsA effect on [Ca^{2+}]$_m$ buffering capacity (Figure 3).

The protective effect of CsA in delaying mPTP opening has long been reported [28,31,32]. Our findings; however, provide the first direct evidence for a novel effect of CsA to enhance the capacity of mitochondria to sequester Ca^{2+} by which it obviates Ca^{2+}-induced mPTP formation. Moreover, the effect of CsA in mediating greater matrix Ca^{2+} buffering explains the sustained free [Ca^{2+}]$_m$ reported by Chalmers and Nicholls [14] and the CsA-induced inhibition of mitochondrial Ca^{2+} efflux observed in other prior studies [33,34].

4.2. Underlying Mechanism of the CsA-Mediated [Ca^{2+}]$_m$ Regulation

It is well established that mitochondria are able to sequester large amounts of Ca^{2+}, while maintaining free [Ca^{2+}]$_m$ over a range of 0.1 and 10 μM depending on the Ca^{2+} load [14]; however, the mechanism and kinetics for this are unclear. Matrix Ca^{2+} buffering capacity is determined by: i) The quantity of Ca^{2+} that can be retained, and ii) the Ca^{2+} threshold level for release when Ca^{2+} exchangers are blocked or maximally operated [48]. The role of P_i as a physiological buffer in regulation of [Ca^{2+}]$_m$ has been extensively studied [14,44,45,49]. The major mechanism of P_i-mediated Ca^{2+} sequestration in mitochondria is believed to be achieved by formation of amorphous Ca^{2+}–P_i complexes in the matrix [48,50,51], which in turn maintain the free [Ca^{2+}]$_m$ at a low level. Hence, sustained [Ca^{2+}]$_m$ cyclically promotes more Ca^{2+} uptake via the MCU due to better preservation of both the Ca^{2+} gradient and $\Delta\Psi_m$.

Though P_i plays an essential role in matrix Ca^{2+} buffering, P_i has also been suggested to induce mPTP opening [52]. A recent study associated Ca^{2+}–P_i precipitation with complex I inhibition and reduced ATP synthase rate during Ca^{2+} overload [53]. Another report demonstrated that increasing [P_i] decreased the mitochondrial Ca^{2+} loading capacity [14]. It was suggested that the mPTP-sensitizing effects of P_i was likely due to its effect in decreasing matrix-free Mg^{2+}, an mPTP inhibitor [20]. In addition, formation of polyphosphate, a known inducer of mPTP, could be a factor in regulating the Ca^{2+} threshold for mPTP activation [54,55]. Interestingly, two prior studies [56,57] indicated that P_i is necessary for the inhibitory effect of CsA on mPTP opening. However, two other studies reported

that CsA inhibits mPTP opening even in the absence of P_i [58,59]. Conversely, in our study, the CsA-induced enhancement of matrix Ca^{2+} buffering was completely annulled when both mitochondria and the experimental medium were depleted of P_i (Figure 7). This loss of Ca^{2+} sequestration by CsA was reinstated when exogenous P_i was added just before activation of the mPTP (Figure 8). These observations provide the essential explanation for the requirement of P_i in the CsA-mediated MCBS and delay in mPTP opening.

The importance of mitochondrial matrix Ca^{2+} buffering via P_i is underscored by the studies of Wei et al. [44,45]. They reported that P_i modulates the total amount of Ca^{2+} uptake with smaller $CaCl_2$ boluses, whereas P_i modulates Ca^{2+} buffering capacity with larger $CaCl_2$ boluses. Since we had P_i in our experimental medium and the mitochondria were replete with exogenous P_i, the observation that CsA induced low $ss[Ca^{2+}]_e$ and $ss[Ca^{2+}]_m$ could be explained by the following: (i) CsA activates P_i-dependent matrix Ca^{2+} buffering potentially by maintaining the rate of Ca^{2+}–P_i complex formation; and (ii) CsA may activate P_i transport processes (via H^+/P_i transporter and/or phosphate carrier) that help to maintain both the IMM pH_m and $\Delta\Psi_m$ gradients. These processes would limit the increase in free $[Ca^{2+}]_m$, which in turn would contribute to more Ca^{2+} uptake and retention by increasing the electrochemical driving force for Ca^{2+} influx.

4.3. CsA vs. ADP; As a Regulator of $[Ca^{2+}]_m$

AdN are implicated as one of the multiple matrix factors responsible for sequestering Ca^{2+} by mitochondria [29,60–62]. AdN can potentiate mitochondrial Ca^{2+} buffering by maintaining high matrix P_i concentrations that can facilitate precipitation of AdN-Ca–P_i complexes, including, ATP-Mg^{2-}/P_i^{2-} and $HADP^{2-}/P_i^{2-}$, and thereby increase the Ca^{2+} threshold for mPTP opening [60,63]. In a study by Carafoli et al. [60], it was reported that mitochondrial Ca^{2+}-buffering is proportional to mitochondrial ADP uptake. In our P_i-replete study, OMN+ADP had a relatively small effect on Ca^{2+} buffering compared to CsA, but it had a significantly larger effect than ADP or OMN alone (Figures 2, 3 and 5). A reasonable explanation could be that OMN, an ATP synthase (Complex V) inhibitor [64], could contribute towards augmenting the AdN pool and thus enhance matrix Ca^{2+} buffering. Consistent with our findings, a previous study also showed a greater CRC with a low-concentration of ADP with OMN compared to 10-fold larger concentration of ADP alone [30]. Thus, in agreement with Sokolova et al. [30], the observed high buffering capacity and expanded CRC with OMN+ADP is largely attributed to the ADP component of the matrix AdN pool. However, a previous study [62] reported that AdN also prevent mitochondrial Ca^{2+} influx by directly chelating Ca^{2+} by a Ca–ATP complexation [61]. Contrary to this observation, in our study, the direct effect of ADP on binding free Ca^{2+} was negligible, as assessed by adding ADP and $CaCl_2$ together in mitochondria-free experimental buffer (Figure S4). Additionally, carboxyatractyloside-mediated inhibition of ADP uptake via adenine nucleotide translocase precluded matrix Ca^{2+} buffering and blunted the CRC by OMN+ADP or ADP alone (Figure S5). In this case, the extra-matrix ADP that accumulated did not chelate the Ca^{2+} added to the buffer. Altogether, these observations indicate that a direct sequestration of Ca^{2+} outside the mitochondria does not explain the effect of ADP alone or OMN+ADP on the enhanced CRC in our study.

A previous study [42] from our group proposed that the MCBS relies on at least two classes of Ca^{2+} buffers. The first class could represent classical Ca^{2+} buffers, including mostly metabolites (ATP, ADP, and P_i) and mobile proteins that bind a single Ca^{2+} ion at a single binding site. A second class of buffers could be associated with the formation of amorphous Ca^{2+} phosphates, which may be capable of binding multiple Ca^{2+} ions at a single site in a cooperative fashion [35,38,39,42]. Genge et al. [65] showed, in an in vitro study, that annexins, a diverse class of proteins, are required for Ca^{2+}-phosphate nucleation. Additionally, many studies have suggested an AdN-dependent Ca^{2+}-binding property of annexins [66]. Interestingly, mitochondria exposed to ADP alone or OMN+ADP retained their ability to maintain low $ss[Ca^{2+}]_e$ and $ss[Ca^{2+}]_m$ for an extended period of cumulative $CaCl_2$ additions, and showed a higher Ca^{2+} threshold for mPTP opening without P_i compared to with P_i (Figure 7). This

extended delay in mPTP opening in the P_i-depleted state compared to the P_i-replete state reflects the ability of P_i to induce early mPTP opening under certain conditions [52]. In this case, the presence of P_i appears to counteract the ADP delay effect and induce a much earlier pore opening compared to the P_i-depleted state. The mechanisms for this AdN-mediated massive matrix Ca^{2+} loading capacity in the absence of exogenous P_i is unclear and needs to be further investigated. A plausible hypothesis could be that, in the absence of P_i, a significant Ca^{2+} loading capacity of AdN might be mediated via direct interaction with annexins. CsA, on the other hand, might function as a mediator that activates a P_i-dependent Ca^{2+} buffering system. Another possibility is that Cyp D, as a PPIase, reduces free phosphate levels in the matrix or blocks the Ca^{2+} binding property of annexins; this then would be relieved by CsA's effect to block Cyp D.

4.4. Implication of CsA-Mediated Ca^{2+} Buffering on Mitochondrial Bioenergetics

Elevated $[Ca^{2+}]_m$ over the nanomolar range is reported to increase NADH generation in part by stimulating Ca^{2+}-sensitive dehydrogenases of the TCA cycle [67,68] and activating the F_0F_1-ATP synthase [69], thereby accelerating oxidative phosphorylation (OXPHOS). However, excess mitochondrial free Ca^{2+} can dissipate $\Delta\Psi_m$ and impede OXPHOS. The IMM $\Delta\Psi_m$ is the key factor in generating the proton motive force across the IMM; it is also one of the primary driving forces for Ca^{2+} uptake via the MCU [70] and triggers Ca^{2+} efflux via the NCLX [71,72]. Therefore, if mitochondria continue to take up Ca^{2+} under increased extra-matrix Ca^{2+} exposure, the Ca^{2+} would have to be buffered or ejected to prevent excess free $[Ca^{2+}]_m$ accumulation that could dissipate $\Delta\Psi_m$ and increase oxidation of NADH.

The stability of Ca^{2+}–P_i precipitates inside the mitochondrial matrix largely depends on pH_m [50]. It is also proposed that the matrix $[P_i]$ depends on the pH gradient (e.g., a change in pH from 7 to 8 has been estimated to increase $[P_i]$ by a factor of 1000 [14,50]). Thus, matrix alkaline conditions could facilitate Ca^{2+}–P_i precipitation, whereas matrix acidification could lead to a destabilization of the Ca^{2+}–P_i precipitate and so enhance matrix free Ca^{2+} levels [14]. Consequently, we correlated the changes in $[Ca^{2+}]_m$ with indices of mitochondrial bioenergetics ($\Delta\Psi_m$, NADH, and pH) (Figure 5) to have a better understanding of the CsA-mediated MCBS. Mitochondria exposed to CsA before the repetitive $CaCl_2$ boluses, exhibited robust mitochondrial Ca^{2+} uptake and rapid $[Ca^{2+}]_m$ buffering while maintaining basal $\Delta\Psi_m$, NADH, and an alkalinized pH_m until mPTP opened (Figure 5). Maintaining $\Delta\Psi_m$ during excess Ca^{2+} uptake in the absence of functioning NCLX suggests a strong matrix buffering effect that is induced by CsA.

In Protocol B, when CsA was added just before the onset of pore opening, NADH and $\Delta\Psi_m$ levels transiently increased but immediately returned to baseline with each added $CaCl_2$ bolus. This transient depolarization and NADH oxidation with each addition of $CaCl_2$ was not observed in Protocol A. The reason for this is unclear. Nonetheless, the observed transient oxidation of NADH helped to restore $\Delta\Psi_m$ after Ca^{2+} induced transient depolarization before the next $CaCl_2$ bolus (Figure 5D,E). The transient redox oxidation and $\Delta\Psi_m$ depolarization suggest that the CsA added at the point just before mPTP opening activated MCBS more slowly compared to Protocol A. In addition, CsA maintained the pH_m gradient during prolonged Ca^{2+} pulse challenges (Figure 5C). This finding also likely excludes a contribution of the mitochondrial calcium–hydrogen exchange (mCHE) to the Ca^{2+} extrusion in the absence of NaCl. We have recently reported that CsA obviates mCHE activity at low extra-matrix pH [19]. However, based on our current results, it is likely that CsA triggered an enhancement of mitochondrial Ca^{2+} buffering so that the resulting low $[Ca^{2+}]_m$ and maintained $\Delta\Psi_m$ and pH_m accounted for the inactivity of mCHE.

5. Conclusions

The salient observation of this study is that CsA mitigated mPTP opening by promoting the maintenance of a low $[Ca^{2+}]_m$, by stimulating and/or potentiating MCBS. Specifically, we showed that the presence of CsA, (i) significantly delayed the mPTP opening when compared to ADP or

OMN+ADP (Protocol A); (ii) overturned the high amplitude increase in $[Ca^{2+}]_m$ (Protocol B); (iii) maintained pH_m, redox state (NADH) and basal $\Delta\Psi_m$, which maintains the driving force for more Ca^{2+} uptake and sequestration; and (iv) activates P_i-dependent mitochondrial Ca^{2+} sequestration to delay mPTP opening.

Our study provides a novel insight into how CsA-mediates a delay in mPTP opening by activating the MCBS, which lowers $ss[Ca^{2+}]_m$ below the threshold for mPTP activation. This concept is shown in the scheme presented in Figure 9. Our finding supports the notion that CsA facilitates P_i-dependent matrix Ca^{2+} buffering, which maintains matrix free Ca^{2+} and enables massive Ca^{2+} loading capacity, without diminishing the driving force for Ca^{2+} influx by maintaining $\Delta\Psi_m$. CsA may delay mPTP opening by enhancing P_i-dependent matrix Ca^{2+} buffering and by inhibiting Cyp D [31,32]. The culmination of these two mechanisms, and possibly others not yet identified, might be responsible for CsA protection against mitochondrial Ca^{2+} overload. Together, these findings add to our understanding of the mechanism of CsA-mediated modulation of mPTP. Importantly, we believe that therapeutic approaches targeted at regulating $[Ca^{2+}]_m$ homeostasis represent a promising strategy to reduce cardiac injury due to Ca^{2+} overload by delaying mPTP opening and preventing induction of apoptosis.

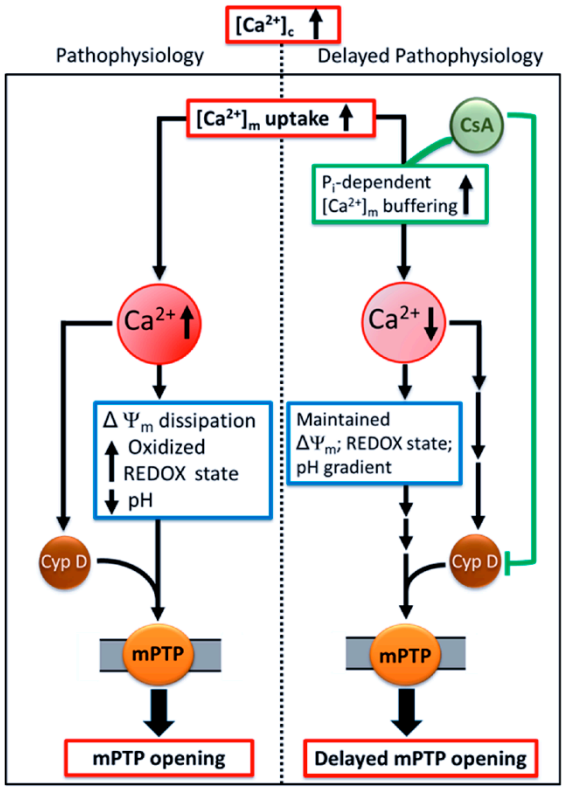

Figure 9. Schema of the potential mechanism by which CsA mediates delay in Ca^{2+}-induced mPTP opening. Pathological conditions, like cardiac ischemia-reperfusion injury, leads to an increase in cytosolic Ca^{2+} ($[Ca^{2+}]_c$). This in turn increases $[Ca^{2+}]_m$ and generation of reactive oxygen species (ROS), impairs respiration and substrate utilization, and leads to uncoupling of oxidative phosphorylation. Lower $\Delta\Psi_m$, oxidized redox state, and dissipation of the pH_m gradient, together induces mPTP opening which triggers apoptosis. These detrimental consequences that underlie IR injury could be mollified by CsA, which allows the mitochondria to maintain their basal $[Ca^{2+}]_m$ via enhanced P_i-dependent matrix Ca^{2+} buffering, in addition to, or through, Cyp D inhibition. Sustained low $[Ca^{2+}]_m$ maintains mitochondrial integrity and function and delays mPTP opening.

Supplementary Materials: The following are available online at http://www.mdpi.com/2073-4409/8/9/1052/s1. Figure S1: Quantification of calcium retention capacity (CRC) for each treatment, DMSO (control), ADP, oligomycin (OMN), OMN+ADP, and CsA during Protocol A (A) and Protocol B (B). Figure S2: Average Ca^{2+} added before mPTP opening, $\Delta\Psi_m$ collapse, NADH oxidation, and matrix acidification. Figure S3: Trend-fits for calculation of buffering rate. Figure S4: Fura-4F ratio representing the change in $[Ca^{2+}]_e$ before and after adding a 20 μM $CaCl_2$ bolus in the absence or presence of 250 μM ADP in the mitochondria-free experimental buffer. Figure S5: Representative raw traces of extra-matrix Ca^{2+} fluorescence (Fura-4F ratio) and Ca^{2+} uptake in mitochondria pretreated with 0.5% DMSO (control), OMN+ADP, and CATR (carboxyatractyloside)+OMN+ADP prior to mPTP opening.

Author Contributions: J.M. and A.K.S.C., conceptualized and designed the experiments; J.M. and A.J.D., performed experiments; J.M., A.J.D. and G.K.N., analyzed data; J.M., W.-M.K., D.F.S. and A.K.S.C., interpreted results; J.M. and A.K.S.C., drafted the manuscript and figures; J.M., G.K.N., W.-M.K., D.F.S. and A.K.S.C., critically read/edited the manuscript. All authors have read and approved the manuscript.

Funding: This project was supported by the Veterans Administration (Merit Review BX-002539-01).

Acknowledgments: The authors are thankful to James S. Heisner for technical assistance.

Conflicts of Interest: The authors declare no conflicts of interest.

References

1. Denton, R.M.; McCormack, J.G. The calcium sensitive dehydrogenases of vertebrate mitochondria. *Cell Calcium* **1986**, *7*, 377–386. [CrossRef]
2. Jouaville, L.S.; Pinton, P.; Bastianutto, C.; Rutter, G.A.; Rizzuto, R. Regulation of mitochondrial ATP synthesis by calcium: Evidence for a long-term metabolic priming. *Proc. Natl. Acad. Sci. USA* **1999**, *96*, 13807–13812. [CrossRef] [PubMed]
3. Bernardi, P. Mitochondrial transport of cations: Channels, exchangers, and permeability transition. *Physiol. Rev.* **1999**, *79*, 1127–1155. [CrossRef] [PubMed]
4. Hajnoczky, G.; Csordas, G.; Das, S.; Garcia-Perez, C.; Saotome, M.; Sinha Roy, S.; Yi, M. Mitochondrial calcium signalling and cell death: Approaches for assessing the role of mitochondrial Ca2+ uptake in apoptosis. *Cell Calcium* **2006**, *40*, 553–560. [CrossRef] [PubMed]
5. Brookes, P.S.; Yoon, Y.; Robotham, J.L.; Anders, M.W.; Sheu, S.S. Calcium, ATP, and ROS: A mitochondrial love-hate triangle. *Am. J. Physiol. Cell Physiol.* **2004**, *287*, C817–C833. [CrossRef] [PubMed]
6. O'Rourke, B.; Cortassa, S.; Aon, M.A. Mitochondrial ion channels: Gatekeepers of life and death. *Physiology (Bethesda)* **2005**, *20*, 303–315. [CrossRef]
7. Camara, A.K.; Lesnefsky, E.J.; Stowe, D.F. Potential therapeutic benefits of strategies directed to mitochondria. *Antioxid. Redox Signal.* **2010**, *13*, 279–347. [CrossRef]
8. Gunter, T.E.; Buntinas, L.; Sparagna, G.; Eliseev, R.; Gunter, K. Mitochondrial calcium transport: Mechanisms and functions. *Cell Calcium* **2000**, *28*, 285–296. [CrossRef]
9. Baughman, J.M.; Perocchi, F.; Girgis, H.S.; Plovanich, M.; Belcher-Timme, C.A.; Sancak, Y.; Bao, X.R.; Strittmatter, L.; Goldberger, O.; Bogorad, R.L.; et al. Integrative genomics identifies MCU as an essential component of the mitochondrial calcium uniporter. *Nature* **2011**, *476*, 341–345. [CrossRef]
10. De Stefani, D.; Raffaello, A.; Teardo, E.; Szabo, I.; Rizzuto, R. A forty-kilodalton protein of the inner membrane is the mitochondrial calcium uniporter. *Nature* **2011**, *476*, 336–340. [CrossRef]
11. Mitchell, P. Coupling of phosphorylation to electron and hydrogen transfer by a chemi-osmotic type of mechanism. *Nature* **1961**, *191*, 144–148. [CrossRef] [PubMed]
12. Mitchell, P. Keilin's respiratory chain concept and its chemiosmotic consequences. *Science* **1979**, *206*, 1148–1159. [CrossRef] [PubMed]
13. Greenawalt, J.W.; Rossi, C.S.; Lehninger, A.L. Effect of Active Accumulation of Calcium and Phosphate Ions on the Structure of Rat Liver Mitochondria. *J. Cell Biol.* **1964**, *23*, 21–38. [CrossRef] [PubMed]
14. Chalmers, S.; Nicholls, D.G. The relationship between free and total calcium concentrations in the matrix of liver and brain mitochondria. *J. Biol. Chem.* **2003**, *278*, 19062–19070. [CrossRef] [PubMed]
15. Starkov, A.A. The molecular identity of the mitochondrial Ca2+ sequestration system. *FEBS J.* **2010**, *277*, 3652–3663. [CrossRef]
16. Carafoli, E.; Tiozzo, R.; Lugli, G.; Crovetti, F.; Kratzing, C. The release of calcium from heart mitochondria by sodium. *J. Mol. Cell. Cardiol.* **1974**, *6*, 361–371. [CrossRef]

17. Palty, R.; Silverman, W.F.; Hershfinkel, M.; Caporale, T.; Sensi, S.L.; Parnis, J.; Nolte, C.; Fishman, D.; Shoshan-Barmatz, V.; Herrmann, S.; et al. NCLX is an essential component of mitochondrial Na+/Ca2+ exchange. *Proc. Natl. Acad. Sci. USA* **2010**, *107*, 436–441. [CrossRef]
18. Boyman, L.; Williams, G.S.; Khananshvili, D.; Sekler, I.; Lederer, W.J. NCLX: The mitochondrial sodium calcium exchanger. *J. Mol. Cell. Cardiol.* **2013**, *59*, 205–213. [CrossRef]
19. Haumann, J.; Camara, A.K.S.; Gadicherla, A.K.; Navarro, C.D.; Boelens, A.D.; Blomeyer, C.A.; Dash, R.K.; Boswell, M.R.; Kwok, W.M.; Stowe, D.F. Slow Ca(2+) Efflux by Ca(2+)/H(+) Exchange in Cardiac Mitochondria Is Modulated by Ca(2+) Re-uptake via MCU, Extra-Mitochondrial pH, and H(+) Pumping by FOF1-ATPase. *Front. Physiol.* **2018**, *9*, 1914. [CrossRef]
20. Bernardi, P.; Vassanelli, S.; Veronese, P.; Colonna, R.; Szabo, I.; Zoratti, M. Modulation of the mitochondrial permeability transition pore. Effect of protons and divalent cations. *J. Biol. Chem.* **1992**, *267*, 2934–2939.
21. Szabo, I.; Zoratti, M. The mitochondrial megachannel is the permeability transition pore. *J. Bioenerg. Biomembr.* **1992**, *24*, 111–117. [CrossRef] [PubMed]
22. Crompton, M. The mitochondrial permeability transition pore and its role in cell death. *Biochem. J.* **1999**, *341 Pt 2*, 233–249. [CrossRef] [PubMed]
23. Kim, J.S.; He, L.; Lemasters, J.J. Mitochondrial permeability transition: A common pathway to necrosis and apoptosis. *Biochem. Biophys. Res. Commun.* **2003**, *304*, 463–470. [CrossRef]
24. Nakagawa, T.; Shimizu, S.; Watanabe, T.; Yamaguchi, O.; Otsu, K.; Yamagata, H.; Inohara, H.; Kubo, T.; Tsujimoto, Y. Cyclophilin D-dependent mitochondrial permeability transition regulates some necrotic but not apoptotic cell death. *Nature* **2005**, *434*, 652–658. [CrossRef] [PubMed]
25. Basso, E.; Fante, L.; Fowlkes, J.; Petronilli, V.; Forte, M.A.; Bernardi, P. Properties of the permeability transition pore in mitochondria devoid of Cyclophilin, D. *J. Biol. Chem.* **2005**, *280*, 18558–18561. [CrossRef] [PubMed]
26. Baines, C.P.; Kaiser, R.A.; Purcell, N.H.; Blair, N.S.; Osinska, H.; Hambleton, M.A.; Brunskill, E.W.; Sayen, M.R.; Gottlieb, R.A.; Dorn, G.W.; et al. Loss of cyclophilin D reveals a critical role for mitochondrial permeability transition in cell death. *Nature* **2005**, *434*, 658–662. [CrossRef]
27. Hunter, D.R.; Haworth, R.A. The Ca2+-induced membrane transition in mitochondria. I. The protective mechanisms. *Arch. Biochem. Biophys.* **1979**, *195*, 453–459. [CrossRef]
28. Halestrap, A.P.; Connern, C.P.; Griffiths, E.J.; Kerr, P.M. Cyclosporin A binding to mitochondrial cyclophilin inhibits the permeability transition pore and protects hearts from ischaemia/reperfusion injury. *Mol. Cell. Biochem.* **1997**, *174*, 167–172. [CrossRef]
29. Haumann, J.; Dash, R.K.; Stowe, D.F.; Boelens, A.D.; Beard, D.A.; Camara, A.K. Mitochondrial free [Ca2+] increases during ATP/ADP antiport and ADP phosphorylation: Exploration of mechanisms. *Biophys. J.* **2010**, *99*, 997–1006. [CrossRef]
30. Sokolova, N.; Pan, S.; Provazza, S.; Beutner, G.; Vendelin, M.; Birkedal, R.; Sheu, S.S. ADP protects cardiac mitochondria under severe oxidative stress. *PLoS ONE* **2013**, *8*, e83214. [CrossRef]
31. Griffiths, E.J.; Halestrap, A.P. Further evidence that cyclosporin A protects mitochondria from calcium overload by inhibiting a matrix peptidyl-prolyl cis-trans isomerase. Implications for the immunosuppressive and toxic effects of cyclosporin. *Biochem. J.* **1991**, *274 Pt 2*, 611–614. [CrossRef] [PubMed]
32. Waldmeier, P.C.; Feldtrauer, J.J.; Qian, T.; Lemasters, J.J. Inhibition of the mitochondrial permeability transition by the nonimmunosuppressive cyclosporin derivative NIM811. *Mol. Pharmacol.* **2002**, *62*, 22–29. [CrossRef]
33. Altschuld, R.A.; Hohl, C.M.; Castillo, L.C.; Garleb, A.A.; Starling, R.C.; Brierley, G.P. Cyclosporin inhibits mitochondrial calcium efflux in isolated adult rat ventricular cardiomyocytes. *Am. J. Physiol.* **1992**, *262*, H1699–H1704. [CrossRef]
34. Wei, A.C.; Liu, T.; Cortassa, S.; Winslow, R.L.; O'Rourke, B. Mitochondrial Ca2+ influx and efflux rates in guinea pig cardiac mitochondria: Low and high affinity effects of cyclosporine A. *Biochim. Biophys. Acta* **2011**, *1813*, 1373–1381. [CrossRef] [PubMed]
35. Blomeyer, C.A.; Bazil, J.N.; Stowe, D.F.; Pradhan, R.K.; Dash, R.K.; Camara, A.K. Dynamic buffering of mitochondrial Ca2+ during Ca2+ uptake and Na+-induced Ca2+ release. *J. Bioenerg. Biomembr.* **2013**, *45*, 189–202. [CrossRef] [PubMed]
36. Aldakkak, M.; Stowe, D.F.; Dash, R.K.; Camara, A.K. Mitochondrial handling of excess Ca2+ is substrate-dependent with implications for reactive oxygen species generation. *Free Radic. Biol. Med.* **2013**, *56*, 193–203. [CrossRef] [PubMed]

37. Agarwal, B.; Dash, R.K.; Stowe, D.F.; Bosnjak, Z.J.; Camara, A.K. Isoflurane modulates cardiac mitochondrial bioenergetics by selectively attenuating respiratory complexes. *Biochim. Biophys. Acta* **2014**, *1837*, 354–365. [CrossRef] [PubMed]
38. Blomeyer, C.A.; Bazil, J.N.; Stowe, D.F.; Dash, R.K.; Camara, A.K. Mg(2+) differentially regulates two modes of mitochondrial Ca(2+) uptake in isolated cardiac mitochondria: Implications for mitochondrial Ca(2+) sequestration. *J. Bioenerg. Biomembr.* **2016**, *48*, 175–188. [CrossRef]
39. Boelens, A.D.; Pradhan, R.K.; Blomeyer, C.A.; Camara, A.K.; Dash, R.K.; Stowe, D.F. Extra-matrix Mg2+ limits Ca2+ uptake and modulates Ca2+ uptake-independent respiration and redox state in cardiac isolated mitochondria. *J. Bioenerg. Biomembr.* **2013**, *45*, 203–218. [CrossRef]
40. Scaduto, R.C., Jr.; Grotyohann, L.W. Measurement of mitochondrial membrane potential using fluorescent rhodamine derivatives. *Biophys. J.* **1999**, *76*, 469–477. [CrossRef]
41. Grynkiewicz, G.; Poenie, M.; Tsien, R.Y. A new generation of Ca2+ indicators with greatly improved fluorescence properties. *J. Biol. Chem.* **1985**, *260*, 3440–3450. [PubMed]
42. Bazil, J.N.; Blomeyer, C.A.; Pradhan, R.K.; Camara, A.K.; Dash, R.K. Modeling the calcium sequestration system in isolated guinea pig cardiac mitochondria. *J. Bioenerg. Biomembr.* **2013**, *45*, 177–188. [CrossRef] [PubMed]
43. Zoccarato, F.; Nicholls, D. The role of phosphate in the regulation of the independent calcium-efflux pathway of liver mitochondria. *Eur. J. Biochem.* **1982**, *127*, 333–338. [CrossRef] [PubMed]
44. Wei, A.C.; Liu, T.; O'Rourke, B. Dual Effect of Phosphate Transport on Mitochondrial Ca2+ Dynamics. *J. Biol. Chem.* **2015**, *290*, 16088–16098. [CrossRef] [PubMed]
45. Wei, A.C.; Liu, T.; Winslow, R.L.; O'Rourke, B. Dynamics of matrix-free Ca2+ in cardiac mitochondria: Two components of Ca2+ uptake and role of phosphate buffering. *J. Gen. Physiol.* **2012**, *139*, 465–478. [CrossRef] [PubMed]
46. Glancy, B.; Balaban, R.S. Role of mitochondrial Ca2+ in the regulation of cellular energetics. *Biochemistry* **2012**, *51*, 2959–2973. [CrossRef] [PubMed]
47. Vasington, F.D.; Murphy, J.V. Ca ion uptake by rat kidney mitochondria and its dependence on respiration and phosphorylation. *J. Biol. Chem.* **1962**, *237*, 2670–2677. [PubMed]
48. Chinopoulos, C.; Adam-Vizi, V. Mitochondrial Ca2+ sequestration and precipitation revisited. *FEBS J.* **2010**, *277*, 3637–3651. [CrossRef] [PubMed]
49. Harris, E.J.; Zaba, B. The phosphate requirement for Ca2+-uptake by heart and liver mitochondria. *FEBS Lett.* **1977**, *79*, 284–290. [CrossRef]
50. Nicholls, D.G.; Chalmers, S. The integration of mitochondrial calcium transport and storage. *J. Bioenerg. Biomembr.* **2004**, *36*, 277–281. [CrossRef]
51. Kristian, T.; Pivovarova, N.B.; Fiskum, G.; Andrews, S.B. Calcium-induced precipitate formation in brain mitochondria: Composition, calcium capacity, and retention. *J. Neurochem.* **2007**, *102*, 1346–1356. [CrossRef]
52. Kushnareva, Y.E.; Haley, L.M.; Sokolove, P.M. The role of low (<or = 1 mM) phosphate concentrations in regulation of mitochondrial permeability: Modulation of matrix free Ca2+ concentration. *Arch. Biochem. Biophys.* **1999**, *363*, 155–162. [CrossRef] [PubMed]
53. Malyala, S.; Zhang, Y.; Strubbe, J.O.; Bazil, J.N. Calcium phosphate precipitation inhibits mitochondrial energy metabolism. *PLoS Comput. Biol.* **2019**, *15*, e1006719. [CrossRef] [PubMed]
54. Abramov, A.Y.; Fraley, C.; Diao, C.T.; Winkfein, R.; Colicos, M.A.; Duchen, M.R.; French, R.J.; Pavlov, E. Targeted polyphosphatase expression alters mitochondrial metabolism and inhibits calcium-dependent cell death. *Proc. Natl. Acad. Sci. USA* **2007**, *104*, 18091–18096. [CrossRef]
55. Seidlmayer, L.K.; Gomez-Garcia, M.R.; Blatter, L.A.; Pavlov, E.; Dedkova, E.N. Inorganic polyphosphate is a potent activator of the mitochondrial permeability transition pore in cardiac myocytes. *J. Gen. Physiol.* **2012**, *139*, 321–331. [CrossRef]
56. Chavez, E.; Moreno-Sanchez, R.; Zazueta, C.; Rodriguez, J.S.; Bravo, C.; Reyes-Vivas, H. On the protection by inorganic phosphate of calcium-induced membrane permeability transition. *J. Bioenerg. Biomembr.* **1997**, *29*, 571–577. [CrossRef] [PubMed]
57. Basso, E.; Petronilli, V.; Forte, M.A.; Bernardi, P. Phosphate is essential for inhibition of the mitochondrial permeability transition pore by cyclosporin A and by cyclophilin D ablation. *J. Biol. Chem.* **2008**, *283*, 26307–26311. [CrossRef] [PubMed]

58. McGee, A.M.; Baines, C.P. Phosphate is not an absolute requirement for the inhibitory effects of cyclosporin A or cyclophilin D deletion on mitochondrial permeability transition. *Biochem. J.* **2012**, *443*, 185–191. [CrossRef]
59. Varanyuwatana, P.; Halestrap, A.P. The roles of phosphate and the phosphate carrier in the mitochondrial permeability transition pore. *Mitochondrion* **2012**, *12*, 120–125. [CrossRef]
60. Carafoli, E.; Rossi, C.S.; Lehninger, A.L. Uptake of Adenine Nucleotides by Respiring Mitochondria during Active Accumulation of Ca++ and Phosphate. *J. Biol. Chem.* **1965**, *240*, 2254–2261.
61. Michailova, A.; McCulloch, A. Model study of ATP and ADP buffering, transport of Ca(2+) and Mg(2+), and regulation of ion pumps in ventricular myocyte. *Biophys. J.* **2001**, *81*, 614–629. [CrossRef]
62. Litsky, M.L.; Pfeiffer, D.R. Regulation of the mitochondrial Ca2+ uniporter by external adenine nucleotides: The uniporter behaves like a gated channel which is regulated by nucleotides and divalent cations. *Biochemistry* **1997**, *36*, 7071–7080. [CrossRef] [PubMed]
63. Traba, J.; Del Arco, A.; Duchen, M.R.; Szabadkai, G.; Satrustegui, J. SCaMC-1 promotes cancer cell survival by desensitizing mitochondrial permeability transition via ATP/ADP-mediated matrix Ca(2+) buffering. *Cell Death Differ.* **2012**, *19*, 650–660. [CrossRef] [PubMed]
64. Devenish, R.J.; Prescott, M.; Boyle, G.M.; Nagley, P. The oligomycin axis of mitochondrial ATP synthase: OSCP and the proton channel. *J. Bioenerg. Biomembr.* **2000**, *32*, 507–515. [CrossRef] [PubMed]
65. Genge, B.R.; Wu, L.N.; Wuthier, R.E. In vitro modeling of matrix vesicle nucleation: Synergistic stimulation of mineral formation by annexin A5 and phosphatidylserine. *J. Biol. Chem.* **2007**, *282*, 26035–26045. [CrossRef] [PubMed]
66. Bandorowicz-Pikula, J.; Buchet, R.; Pikula, S. Annexins as nucleotide-binding proteins: Facts and speculations. *Bioessays* **2001**, *23*, 170–178. [CrossRef]
67. McCormack, J.G.; Denton, R.M. Intracellular calcium ions and intramitochondrial Ca2+ in the regulation of energy metabolism in mammalian tissues. *Proc. Nutr. Soc.* **1990**, *49*, 57–75. [CrossRef] [PubMed]
68. Rutter, G.A. Ca2(+)-binding to citrate cycle dehydrogenases. *Int. J. Biochem.* **1990**, *22*, 1081–1088. [CrossRef]
69. Territo, P.R.; Mootha, V.K.; French, S.A.; Balaban, R.S. Ca(2+) activation of heart mitochondrial oxidative phosphorylation: Role of the F(0)/F(1)-ATPase. *Am. J. Physiol. Cell Physiol.* **2000**, *278*, C423–C435. [CrossRef] [PubMed]
70. Chinopoulos, C.; Adam-Vizi, V. The 'ins and outs' of Ca2+ in mitochondria. *FEBS J.* **2010**, *277*, 3621. [CrossRef] [PubMed]
71. Jung, D.W.; Baysal, K.; Brierley, G.P. The sodium-calcium antiport of heart mitochondria is not electroneutral. *J. Biol. Chem.* **1995**, *270*, 672–678. [CrossRef] [PubMed]
72. Kim, B.; Matsuoka, S. Cytoplasmic Na+-dependent modulation of mitochondrial Ca2+ via electrogenic mitochondrial Na+-Ca2+ exchange. *J. Physiol.* **2008**, *586*, 1683–1697. [CrossRef] [PubMed]